Climatological evolution and interannual variation of the Okinawa baiu

Yasuko Okada

Division of Earth System Science,

Graduate School of Environmental Earth Science,

Hokkaido University

August, 2012

Abstract

The Okinawa baiu (summer rainy season) starts in early May and ends in late June, preceding the baiu in mainland Japan by approximately one month. This study investigates the time evolution of the large-scale circulation associated with the Okinawa Baiu using 10-year (1997–2006) climatologies of precipitation and meteorological fields, with particular focus on temperature advection at 500 hPa. We also investigate the interannual variation during the Okinawa baiu using the above dataset over a longer time period (1979-2008).

The onset of the Okinawa baiu occurs in early May, and is followed by an initial peak in precipitation during mid-May. The baiu rainband then moves southeastward, leading to a short break in baiu precipitation during late May. The rainband returns to Okinawa in early June, and a second peak in precipitation occurs during mid-June. The baiu rainband withdraws northward in late June.

The mid-May precipitation peak is associated with warm advection at 500 hPa, mainly due to the meridional temperature gradient and the prevailing southerly winds. This warm advection coincides with upward motion near Okinawa; however, the warm advection is insufficient to explain the peak precipitation amount. Enhancement of precipitation by a transient disturbance probably contributes to the peak amount. The break period during late May coincides with the peak of South China Sea monsoon. Warm advection at 500 hPa strengthens again in June because of the strong zonal thermal contrast between the warm Tibetan Plateau and cold Pacific. This warm advection is able to adequately explain both the upward motion and precipitation. These results indicate that the large-scale meteorological characteristics are different during the first and second peaks.

Interannual variability of Okinawa baiu is examined for May and June, focusing on the 500-hPa temperature advection. The temperature, wind, and advection fields related to the Okinawa baiu are generally consistent with the climatological analysis. Namely, the southerly temperature advection is weakly related with the precipitation amount in May, while the zonal warm advection is significantly correlated with that in June. Moreover, it is found that Okinawa baiu in June is enhanced in El Nino years, while that in May has no association with ENSO. The relation with the PJ pattern is not found both in May and June.

These results support our interpretations of differences between large-scale features associated with the Okinawa baiu in May and those associated with the Okinawa baiu in June.

Acknowledgments

I would like to express greatly appreciation to Professor Koji Yamazaki for helpful discussion and advise which is reflected to this dissertation. The member of this dissertation committee, Professor Fumio Hasebe, Associate professor Masatomo Fujiwara, Associate professor Takeshi Horinouchi and Associate professor Masaru Inatsu, gave me many helpful comments and suggestions. I also wish to express my gratitude to Associate Professor Youichi Tanimoto, gave me many insightful comments in academic conferences or informal seminars.

I received much helps and support from the staffs and members of Atmospheric Science, Graduate School of Environmental Earth Science, Hokkaido University. They gave me the skill, motivation, encouragements, and pleasant student life. Special thanks go to Dr. Kazuhiro Oshima, Dr. Yumiko Yara, Dr. Hiroshi Koyama, Mr. Jun Ohtake, Mr. Takatoshi Sakazaki, Mr. Akira Ooshima, Ms. Rie Muranaka and all of women in “Ouoku”.

I also would express my gratitude to all the members and old-members of Yamazaki laboratory for their useful comments and beneficial discussions. I would like to thank Mr. Nobuyuki Kayaba of the Japan Meteorological Agency for supporting the LBM calculations.

The JRA-25 atlas was made by the JRA-25 long term re-analysis project that Meteorological Agency and Central Res. Inst. of Electric Power Industry Foundation carried out. The GrADS is used for analysis and drawing figures.

Finally, I would like to thank my parents for support my student life.

Contents

List of Figures

List of Table

Chapter 1

Introduction

Between May and July, East Asia experiences a rainy season that is known as the meiyu in China and as the baiu in Japan. Okinawa is located southwest of mainland Japan on the eastern fringe of the East China Sea, and consists of numerous small islands (see Fig. 1.1). In this study, we define the “Okinawa region” as the region within 23°–28°N and 123°–129°E. The Okinawa baiu starts in May when the baiu rainband, which is first observed in late April as a band of enhanced cloudiness along a polar front near 30°N, shifts southward to approximately 20°–25°N (Tanaka 1992). Tian and Yasunari (1998) examined the occurrence of persistent rains over central China during spring (March and April), and showed that this area of precipitation moves southward in May. The baiu rainband moves rapidly northward in June. This rapid northward shift leads to quasi-stationary precipitation and the onset of the meiyu–baiu season over a broad region of East Asia, from southern China to mainland Japan (Kato 1985; Tanaka 1992). The baiu front continues to move northward, withdrawing from mainland Japan in mid-July. This continued northward movement is associated with the concurrent northward shift of the upper-level jet. Ueda et al. (1995) suggested that abrupt changes in convective activity over the northwestern Pacific during late July are associated with the northward withdrawal of the baiu front.

The meiyu-baiu rainband is characterized by a frontal structure in the lower troposphere, which is called the meiyu-baiu front. That can be identified as sharp gradients in specific humidity and potential temperature (Matsumoto et al. 1971). The front differs in its characteristic to the east and west of 120°–130°E. To the east, the temperature gradient across the front is strong; to the west, the temperature gradient is weaker but the moisture gradient is stronger (Matsumoto et al. 1971; Kato 1985; Ninomiya and Muraki 1986; Ninomiya and Akiyama 1992). Eastward of 120°–130°E, the baiu front describes the boundary between a warm subtropical airmass to the south and a cold subpolar airmass to the north. To the west, over China, the front describes the boundary between a humid tropical airmass to the south and a dry subpolar airmass to the north (Tanaka 2007). Okinawa is located at 123°–129°E, within the transitional zone between the temperature-gradient front region (to the east) and the moisture-gradient front region (to the west).

Figure 1.1 shows the May–June evolution of the 297 K isotherm in surface air temperature as a series of 5-day averages for 10 years from 1997 through 2006. During May, the 297 K isotherm is located just north of Okinawa and is oriented roughly east–west, running from southern China to the Pacific Ocean. In early June, an abrupt warming occurs over China and a more gradual warming occurs eastward of 120°–125°E. This distribution of warming leads to the formation of a zonal temperature contrast between continental China and the East China Sea.

Figures 1.2 and 1.3 show the time evolution of climatological north–south gradients in potential temperature and specific humidity at 925 hPa averaged over the longitudinal range that contains Okinawa (123°–129°E). The meridional temperature gradient near Okinawa is strong throughout boreal winter (Fig. 1.2). The strongest temperature

gradient in this longitudinal range is located near 24°–29°N until mid-June, although its magnitude weakens slightly during June (Fig. 1.3a). The strongest moisture gradient is also located at approximately 25°–30°N until mid-June, when it moves northward (Fig. 1.3b). The Okinawa baiu front is characterized by strong gradients in both temperature and moisture.

The meiyu-baiu rainband is also characterized by a pressure contrast between a planetary-scale surface low over the China and a high over the Northwest Pacific, with southerly winds prevailing along the east coast in meiyu-baiu season (Fig. 1.4b). However, this contrast does not exist in May, and a subtropical high stretches to China with southeasterly wind (Fig. 1.4a).

The extensive studies about the meiyu-baiu season exist (Ninomiya and Akiyama 1992; Kodama 1992; Ninomiya and Shibagaki 2007, and references therein) but they do not show clearly why the baiu front appears at specific location and time.

Sampe and Xie (2010) explained the large-scale dynamics of the baiu rainband from the perspective of temperature advection in the mid-troposphere. Warm advection implies upward motion in adiabatic flow. During the baiu season in East Asia, the zonal contrast of temperature in the mid-troposphere is enhanced due to warming of the Asian continent, especially that of the Tibetan Plateau. The prevailing westerly wind is also relatively strong, which promotes strong warm advection toward East Asia. This region of strong warm advection corresponds well to the region of upward motion along the baiu front. In this paper, we apply the hypothesis proposed by Sampe and Xie (2010) to the Okinawa baiu.

The evolution of the Okinawa baiu precedes the evolution of the baiu in mainland Japan by approximately one month, with onset in early May and withdrawal in late June

(climatological values from the Japan Meteorological Agency indicate an average onset date of 8 May and an average withdrawal date of 23 June). In early May, Okinawa is usually located at the southern edge of a moving high-pressure system. The spring rainy season, which extends from mid-March to early May, is caused by extratropical cyclones and frontal systems in the Japanese Nansei-Shotou (southwest islands) (Matsumoto and Yamamoto 2009). The onset of the Okinawa baiu takes place when the east–west front associated with the moving high-pressure system becomes stationary. The westerly winds are still strong at this time; accordingly, moist air intrusions and precipitation events are intermittent during May, and the amount of rainfall is relatively small (Ishigaki 1982). A cloud zone appears over subtropical East Asia at approximately the same time (Hirasawa et al. 1995). Precipitation amounts increase in June, corresponding to the duration of the baiu from mid-May to mid-June (Matsumoto and Yamamoto 2009). The Okinawa baiu ends in late June with the northward shift of the baiu front.

The meiyu-baiu rainband over East Asia displays large interannual variability. Kosaka et al. (2011) analyzed the interannual variability and revealed that precipitation anomalies over the meiyu-baiu region are accompanied by anomalies of mid-tropospheric horizontal temperature advection using a singular value decomposition (SVD) analysis. They showed that a warm (cool) advection causes increased (decreased) meiyu-baiu precipitation locally by inducing adiabatic ascent (decent). The precipitation acts to reinforce the vertical motion, forming a feedback system. They also showed the association of meiyu-baiu precipitation with the Pacific-Japan (PJ) teleconnection pattern. This pattern is known as the significant correlation between atmospheric pressure of the East Asia and strength of convection around Philippine

(Nitta 1987; Kosaka and Nakamura 2010; Hirota and Takahashi 2012). The PJ pattern mediates influences of the El Nino-Southern Oscillation (ENSO) in preceding boreal winter on meiyu-baiu precipitation. However, these results do not show the relationship with pre- meiyu-baiu season in May.

Although the temporal evolution and interannual variability of the baiu over mainland Japan has been extensively studied, few studies have examined the evolution of the Okinawa baiu. Previous analyses of the Okinawa baiu (e.g., Ishigaki 1982) have been based on monthly averages; its evolution has not yet been studied using daily data. In this study, we provide a detailed examination of the climatological evolution of the Okinawa baiu, with particular focus on temperature advection at 500 hPa.

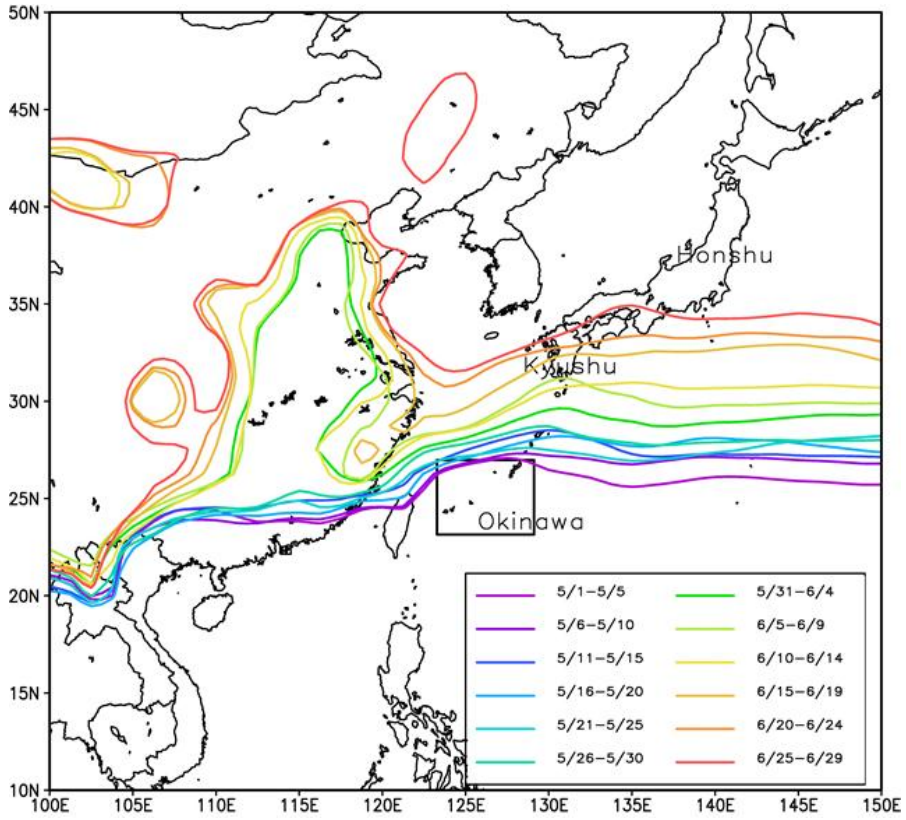

Figure 1.1: Contour lines indicate the climatological location of the 297 K surface air temperature isotherm for successive pentads during May and June. The solid rectangle in the map indicates the Okinawa region, and the legend is shown at the bottom right.

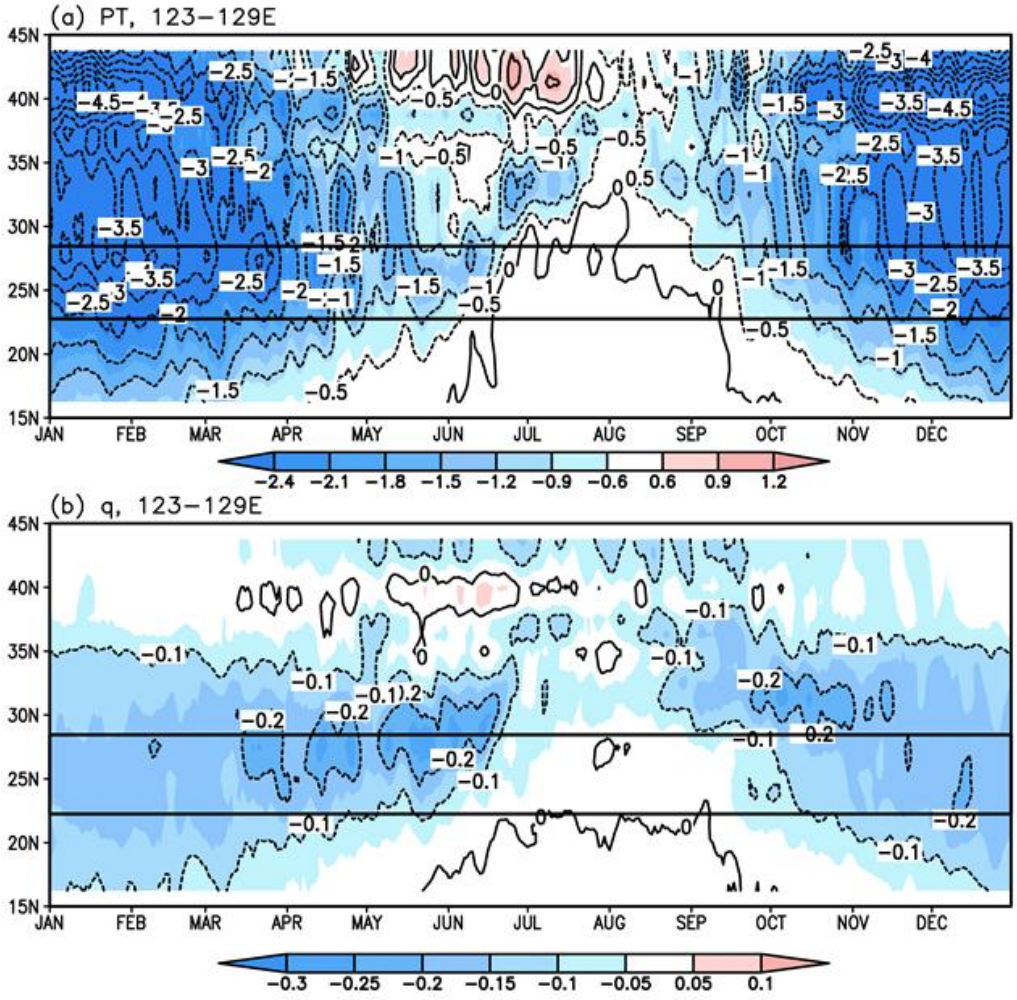

Figure 1.2: Time–latitude plots of meridional gradients in (a) potential temperature (K) and (b) specific humidity (kg kg^{-1}) at 925 hPa averaged over the longitudinal range 123°–129°E from 1 January to 31 December. The black horizontal lines indicate the boundaries of the Okinawa region.

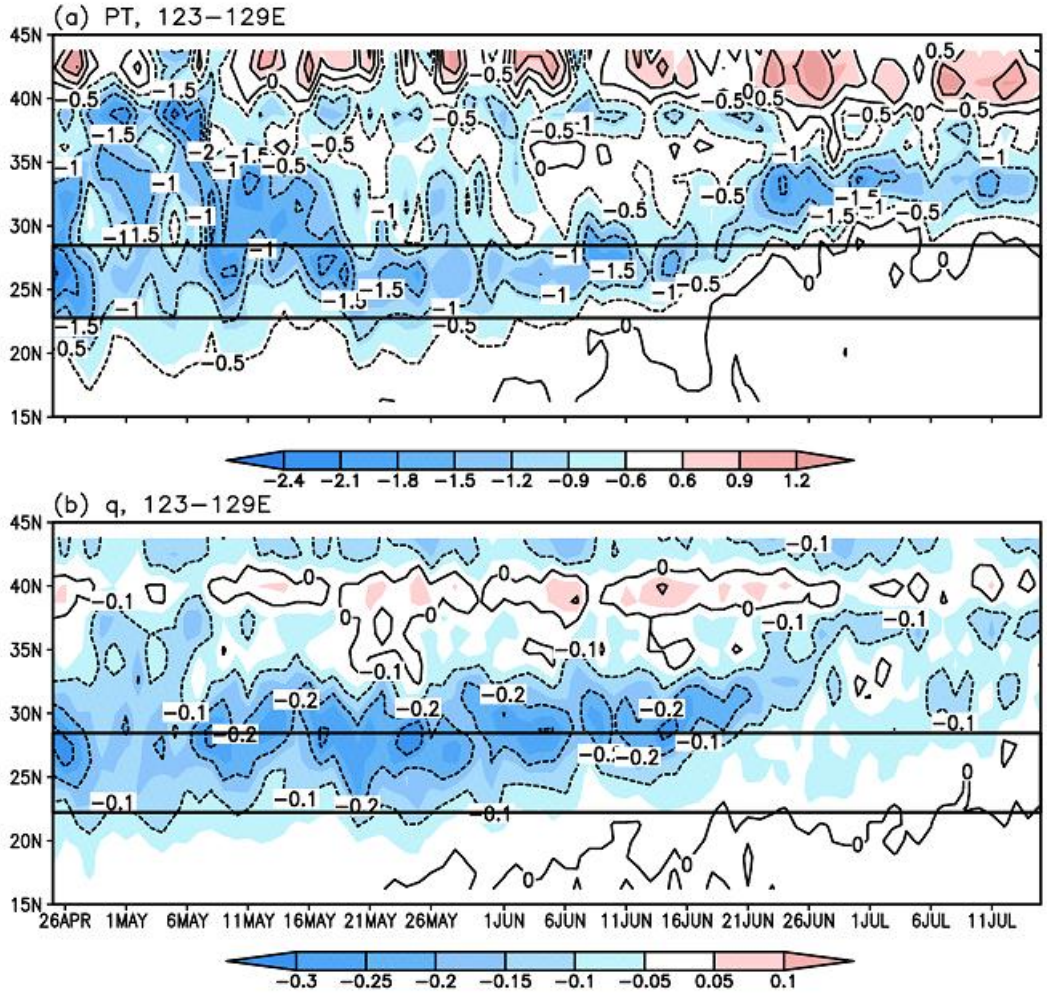

Figure 1.3: Same as Figure 1.2 but for period with from 25 April to 15 July.

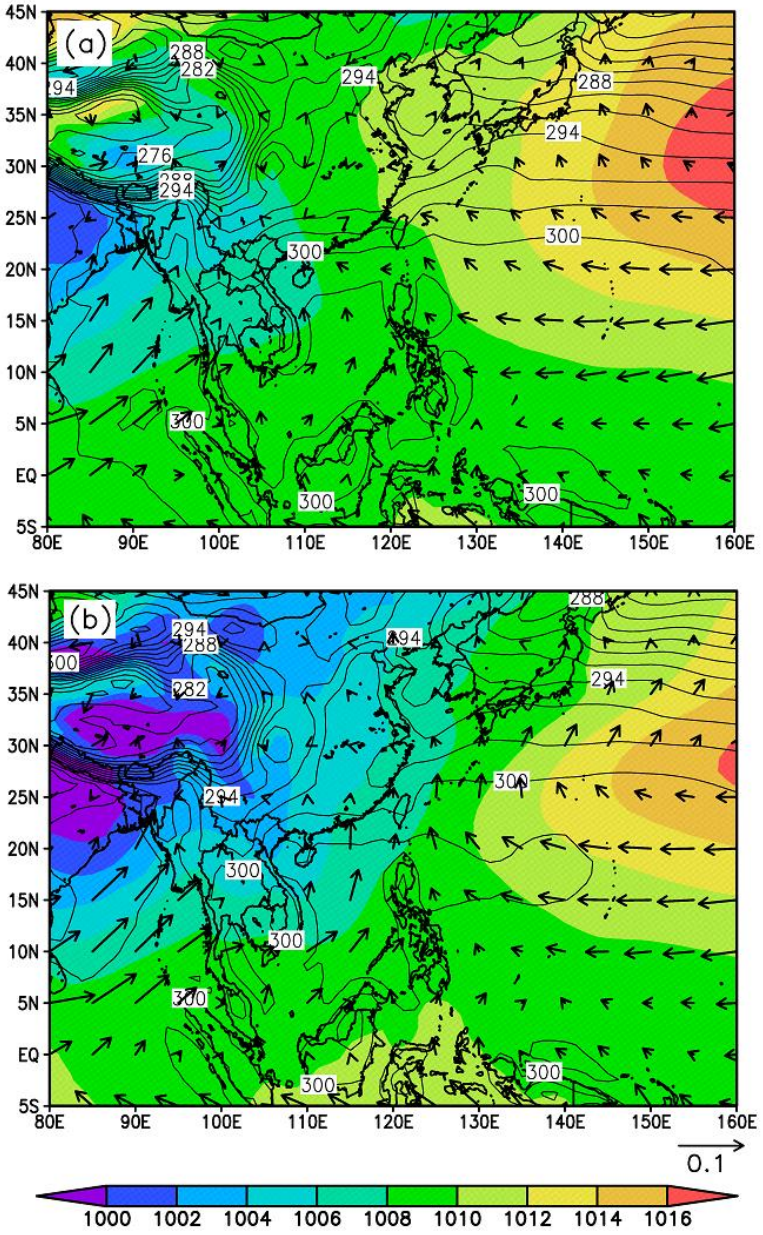

Figure 1.4: Climatology of sea level pressure (color; hPa), surface air temperature (contour at every 2 K) and surface wind (arrows; m s^{-1}). (a) May. (b) June.

Chapter 2

Data

We use meteorological data from the Japanese 25-year Reanalysis (JRA-25) (Takahashi et al. 2006; Onogi et al. 2007; Watarai and Tanaka 2007) and precipitation data from the Global Precipitation Climatology Project (GPCP) (Huffman et al. 2001) for the 10 years from 1997 through 2006. The JRA-25 dataset is provided 6-hourly at a horizontal resolution of 1.25° × 1.25° (longitude × latitude). The GPCP data is provided daily at a horizontal resolution of 1° × 1° over the entire globe for the period October 1996 - present. This data set is made by infrared channel data and microwave channel data, which observed by geostationary operational environmental satellite and polar orbit satellite, and ground-based observation data. We use the Asian Precipitation—Highly Resolved Observational Data Integration Towards Evaluation of Water Resources (APHRODITE) precipitation dataset (Yatagai et al. 2009) to supplement the GPCP data. The APHRODITE data is based solely on rain-gauge observations, and is therefore only available over land. This dataset is provided daily at a horizontal resolution of 0.5° × 0.5°. We use sea surface temperatures from the NOAA 1/4 degree daily Optimum Interpolation Sea Surface Temperature (OISST) dataset (Reynolds et al. 2007; Reynolds 2008). The OISST data is provided daily at a horizontal resolution of 0.25° × 0.25°. We define the “Okinawa region” as the region within 23°–

28°N and 123°–129°E. All results shown in Chapter 3 are 10-year means over the period 1997–2006, because of the GPCP data is from October 1996.

In Chapter 4, we also used the following monthly data to examine an interannual variability; the meteorological data from the Japanese 25-year Reanalysis (JRA-25) (Takahashi et al. 2006; Onogi et al. 2007; Watarai and Tanaka 2007) and precipitation data from the Global Precipitation Climatology Project (GPCP) version 2.1 (Huffman et al. 2001) for the 30 years from 1979 through 2008. The JRA-25 dataset is provided 6-hourly at a horizontal resolution of 1.25° × 1.25° (longitude × latitude) and the monthly data is calculated from the original 6-hourly data. The GPCP data is provided monthly at a horizontal resolution of 2.5° × 2.5°. We use sea surface temperatures from the Hadley Centre Ice and Sea Surface Temperature (HadISST) dataset (Rayner et al. 2003). The HadISST data is provided monthly at a horizontal resolution of 1° × 1°. We define the “Okinawa region” as the region within 23°–28°N and 123°–129°E as in the Chapter 3.

Chapter 3

Baiu season evolution of meteorological fields

3.1 Precipitation and sea level pressure

The climatological onset date of the Okinawa baiu is 8 May, and the climatological withdrawal date is 23 June (climatological values based on the 30-year period from 1971 through 2000 as reported by the Japan Meteorological Agency). The average onset and withdrawal dates for the 10-year period analyzed in this paper match these climatological values: the average onset date is 8 May and the average withdrawal date is 23 June. The baiu rainband displays large variability temporally. Figure 3.1 shows the time series of precipitation over the Okinawa region for each year from 25 April to 15 July. Though the variability of precipitation is large, Fig. 3.1 shows a tendency to have the first peak in mid-May, short break in late-May, and the second peak in mid-June. Figure 3.2 shows the temporal evolution of smoothed daily mean precipitation climatology with standard deviation and error. The difference between the peak in mid-May and the minimum in late-May is statistically significant at 95 % level. In addition, the difference between the minimum in late-May and the peak in mid-June is statistically significant at 95 % level. Figure 3.3a shows the temporal evolution from 25 April to 15 July of GPCP and APHRODITE precipitation averaged over the Okinawa

region. According to GPCP, precipitation starts to increase around 10 May, reaching a peak of approximately 12 mm day^{-1} around 18 May. Precipitation decreases following this mid-May peak, reaching a minimum of approximately 4 mm day^{-1} around 26 May, after which it increases again. Precipitation reaches a seasonal maximum of approximately 13 mm day^{-1} between 6–12 June. This seasonal maximum is both larger and longer lasting than the initial peak in mid-May. Precipitation decreases following the peak in mid-June, and the Okinawa baiu ends around 23 June. APHRODITE data indicates that the mid-May precipitation peak is slightly earlier (around 15 May) and smaller (approximately 10 mm day^{-1}). The subsequent minimum (4 mm day^{-1}) also occurs earlier, around 22 May. The secondary peak in June is somewhat stronger than that indicated by GPCP, with a maximum of approximately 15 mm day^{-1}. The APHRODITE data indicates that the Okinawa baiu ends around 21 June. The temporal evolution of precipitation is generally similar in the GPCP and APHRODITE datasets, despite slight differences in key dates and precipitation amounts. Such differences are unavoidable because the APHRODITE data is only available over land. The land area of the Okinawa islands is much smaller than the area of the Okinawa analysis region defined above. In summary, the Okinawa baiu has two periods of peak precipitation, one in mid-May and the other in mid-June. A short break period occurs during late May, between the two peak periods.

The time–latitude evolution of precipitation averaged over the longitudinal range 123°–129°E is shown in Fig. 3.3b. Precipitation amounts near 27°N increase gradually during early May, as the region of high precipitation moves southward over Okinawa. This region of high precipitation continues southward during late May, leading to a short break in the Okinawa baiu. In June, the precipitation zone moves northward and

precipitation amounts increase. The region of high precipitation reaches 30°–35°N in late June, at which point it becomes nearly stationary. Based on these observations of the evolution of the Okinawa baiu, we divide the May–June period into 5-day increments (pentads). The following figures show horizontal distributions of a variety of meteorological fields during successive pentads.

Figure 3.4 shows the distribution of pentad-mean precipitation and sea level pressure (SLP) for each pentad during the evolution of the Okinawa baiu. In early May (pre-onset), the largest precipitation is observed near the equator, with weak precipitation south of the Yangtze River valley in China (~28°N) (Fig. 3.4a–b). The axis of the North Pacific subtropical high (NPSH) is located near 30°N and extends westward to China.

In mid-May, an area of high precipitation forms that extends from the Yangtze River valley in the west through Kyushu island and the Okinawa region in the east (Fig. 3.4c). Precipitation is also significantly enhanced over the Bay of Bengal (BOB, 85°–95°E). A precipitation zone forms in mid-May that extends from Southern China to the east of Japan, corresponding to the onset of the Okinawa baiu (Fig. 3.4d). Monsoon onset occurs over the Indochina Peninsula (~105°E) during this first period of peak precipitation. The NPSH retreats eastwards, and the ridge of the NPSH is oriented southwest–northeast. The main precipitation zone is located along the northwestern side of this ridge.

In late May, the NPSH continues its eastward retreat and the precipitation moves southward over the South China Sea (SCS, 110°–120°E) (Fig. 3.4e–f). This southeastward migration of the precipitation area corresponds to monsoon onset over the SCS and causes a short break in the Okinawa baiu at the end of May (Figs 3.3 and

3.4e-f). Fujibe (2006) found that a short dry period precedes baiu onset over Honshu–Kyushu, and suggested that Okinawa may experience a similar short break in precipitation during late April. We instead find that this short break occurs during late May. In their examination of the baiu front in May 1979, Kato and Kodama (1992) showed that the front moved southeastward from Okinawa in late May (see their fig. 15). This southeastward migration during late May is consistent with our results (Figs. 3.3 and 3.4).

The precipitation zone returns to the Okinawa region in early June as part of a precipitation belt that is oriented southwest–northeast and extends from the northern SCS to the east of Honshu Island (Fig. 3.4g–h). The maximum precipitation amounts along this belt are located between Okinawa and Kyushu Island. Precipitation increases gradually over the BOB (Fig. 3.4g–j) and along the west coast of India (not shown) during this period. Using 27-year (1979–2006) climatological pentad-mean rain rates, Ueda et al. (2009) explained this stepwise evolution of precipitation in Asia as the seasonal progression of precipitation along the 10°–20°N latitudinal band. Matsumoto (1997) also showed this stepwise evolution of precipitation over Indochina and the adjacent monsoon region using pentad-mean observations of outgoing long-wave radiation (OLR).

The Okinawa baiu withdraws in late June (Fig. 3.4k–l). The precipitation zone, which was located over Okinawa during the previous period, shifts northward so that the areas of peak precipitation are centered over the Yangtze River basin and Kyushu islands. This northward shift is associated with the westward expansion of the NPSH into the Okinawa region (Fig. 3.4k–l). Precipitation increases southward of the NPSH (near 5°–10°N) during this period.

3.2 Moisture flux and precipitable water

Low-level water vapor transport into the frontal zone by monsoon winds is essential to the formation of baiu precipitation (Ninomiya and Akiyama 1992; Tanaka 2007). Figure 3.5 shows the spatial distributions of moisture flux integrated from the surface to 200 hPa (arrows), moisture flux convergence (color shading), and precipitable water (contours). The moisture fluxes $\langle q\mathbf{v} \rangle$ are vertically integrated from the surface to 200 hPa, expressed as follows:

$$\langle q\mathbf{v} \rangle = \frac{1}{g} \int_{200hPa}^{ground} \mathbf{V} \cdot q dp \quad . \qquad (1)$$

Although the moisture flux is integrated throughout the troposphere, water vapor is most abundant in the lower troposphere. The direction of the flux therefore primarily reflects low-level moisture transport.

The moisture flux is southwesterly over southern China and regions to its east during early May (Fig. 3.5a), with areas of weak moisture flux convergence in southern China. The moisture flux is easterly from the northwestern subtropical Pacific to the SCS.

Westward fluxes continue to prevail over the northwestern subtropical Pacific through mid-May (Fig. 3.5b). These westward fluxes are directed toward the Indochina Peninsula along the southern periphery of the NPSH. A weak northward flux prevails over the SCS, with moisture flux convergence to the east of the Philippines. In mid-May, coincident with the first peak in Okinawa baiu precipitation, a southwesterly moisture flux develops over the BOB. This southwesterly moisture flux connects with southwesterly fluxes over southern China and Okinawa. Areas of moisture flux convergence are observed over Indochina and southern China; these areas extend

toward Okinawa.

During the Okinawa baiu break period (late May), precipitable water exceeds 50 mm over an area that extends across the northern SCS from southern China along 20°–25°N (Fig. 3.5c). Precipitation is suppressed to the south of this humid band, along the ridge axis of the NPSH (15°N~25°N). The westerly moisture flux over the SCS strengthens at this time and the SCS monsoon becomes strong (Chan et al. 2000). Wang et al. (2004) showed that the mean 850-hPa westerly wind over the central SCS (5°–15°N, 110°–120°E; U_{SCS}) strengthens at the onset of the SCS monsoon. They used this information to define SCS monsoon onset as the first pentad after 25 April that satisfies the following two criteria: U_{SCS} is positive in the onset pentad and at least two of the following three pentads, and U_{SCS} averaged over the four pentads exceeds 1 m s^{-1}. According to this definition, SCS monsoon onset typically occurs around 15 May during our analysis period. U_{SCS} peaks at approximately 25 May (not shown). We also find that the break period of the Okinawa baiu occurs simultaneously with the peak of the SCS monsoon. The moisture flux southeast of Okinawa is directed toward the northeast, leading to moisture convergence and an eastward extension of the region of high precipitable water (Fig. 3.5c).

We have also investigated the response of the atmospheric circulation to convective heating under climatological mean conditions for May using the linear baroclinic model (LBM) (Watanabe and Kimoto 2000), with particular focus on the relationship between the Okinawa baiu and the SCS monsoon. The introduction of an idealized heat source to the west of the Philippines (15°N, 110°E) induces a low-level cyclonic circulation westward of 115°E and a low-level anticyclonic circulation eastward of 115°E (Fig. 3.6, N. Kayaba, 2012, personal communication). The latter includes the Okinawa region.

This result suggests that convection over the SCS acts to suppress precipitation over Okinawa and to the east of the Philippines, and supports our conclusion that the short break in the Okinawa baiu during late May is related to the onset of the SCS monsoon. This explanation cannot explain the southeastward shift in the precipitation area near Okinawa, however. Changes in the distribution of transient disturbances probably play a role in this southeastward shift (section 3.5).

The westerly moisture flux over the SCS shifts to southwesterly during early June (Fig. 3.5d–e). This southwesterly moisture flux provides an abundant supply of water vapor and promotes precipitation in the Okinawa region. Moisture convergence along the baiu front increases substantially and the front moves slowly northward as the monsoon circulation in Southeast Asia gradually strengthens during early and mid-June (Fig. 3.5e). This northward movement continues into late June, resulting in the end of the Okinawa baiu (Fig. 3.5f). The zone of strong moisture convergence over China shifts northward into central China. The areas of moisture convergence (Fig. 3.5) correspond approximately to areas of precipitation (Fig. 3.4) throughout May and June.

3.3 Horizontal temperature advection

Throughout the rainy season, mean ascending motion along the baiu front corresponds well to a band of warm horizontal temperature advection in the mid-troposphere (Sampe and Xie 2010). The response of the large-scale atmospheric circulation to diabatic heating from condensation is generally baroclinic; as a result, the mid-tropospheric circulation is not strongly affected by this heating. Sampe and Xie (2010) examined temperature advection at the 500-hPa level and found good correlations between warm advection and precipitation during the baiu season. We now

examine in detail whether this relationship applies to the Okinawa baiu. In the present study, we used the thermodynamic energy equation in pressure coordinates, expressed as follows:

$$\frac{\partial T}{\partial t} = \frac{Q}{C_p} - \left(\frac{p}{p_0}\right)^{R/C_p} \omega \frac{\partial \theta}{\partial p} - \mathbf{v} \cdot \nabla_p T , \qquad (2)$$

where Q is diabatic heating/cooling, p_0 a standard constant pressure (=1000 hPa), and other notations are standard. The horizontal temperature advection of the third term on the right is calculated from 6-hourly data before averaging over 10 years.

Figure 3.7 shows the 500-hPa horizontal temperature advection (contours) and upward vertical pressure velocity ($-\omega$; color shading). Warm advection roughly corresponds to ascending motion outside of the tropics. The transient term of temperature advection has only small effects on the Okinawa baiu. Figure 3.8 shows the temporal evolution of upward vertical velocity ($-\omega$) and horizontal temperature advection at 500 hPa near Okinawa. Variations in ascending motion and warm advection correspond reasonably well to variations in areas of precipitation associated with the Okinawa baiu (compare Figs 3.3 and 3.8b). In particular, the region of warm advection shifts southeastward during the short break in the baiu during late May (Figs 3.7c and 3.8b). At around the same time, the cold advection located to the north extends southward to cover the north of Okinawa. During the second peak in baiu precipitation, the temperature advection over the Okinawa region increases only slightly (from approximately 0.3 K day^{-1} to approximately 0.4 K day^{-1}), while the upward pressure velocity increases by a factor of 1.5. Decreases in static stability (see section 3.4) and increases in diabatic heating due to condensation likely contribute to the relatively large increase in vertical pressure velocity during mid-June relative to that during May. On

the other hand, in May, magnitudes of warm advection and vertical p-velocity are insufficient to explain the precipitation peak. In addition, we compared vertical advection term to horizontal temperature advection term of expression (2) in May and June. In May, cooling by the vertical advection (K day^{-1}) is about 1.2 times larger than warming by horizontal advection (K day^{-1}), which means two terms are nearly balanced. On the other hand, in June, cooling by the vertical advection is about 1.7 times larger than warming by horizontal advection, which means diabatic heating play an important role for inducing ascent in June.

Sampe and Xie (2010) showed that the westerly jet stream across the zonal temperature gradient contributes to ascending motion and the formation of the baiu front. Figure 3.9 shows horizontal wind, temperature, and temperature advection at 500 hPa. During early May, the warmest temperatures are located over the BOB. This region moves northward as the season progresses, so that it is located over the Tibetan Plateau in late June. Matsumoto (1992) showed that warming over the Tibetan Plateau influences the seasonal transitions that occur over Japan during mid-May and mid-June. The meridional temperature gradient near Okinawa is large during May, so that the southerly component of wind contributes to temperature advection even though it is relatively weak (Fig. 3.9a). Cold advection associated with the trough near Korea prevails in the area north of Okinawa (Fig. 3.9b–c). The zonal temperature contrast near Okinawa strengthens during June, as does temperature advection associated with westerly wind (Fig. 3.9d–e). The region of warm temperature advection shifts northward from Okinawa during late June, when the Okinawa baiu withdraws (Fig. 3.9f). Warm advection and upward motion both approach zero at this point (Fig. 3.8).

We divide temperature advection into its zonal and meridional terms according to

$$-\mathbf{v}\cdot\nabla T = -u\frac{\partial T}{\partial x} - v\frac{\partial T}{\partial y} \qquad (3)$$

Figure 3.10 shows the zonal term of temperature advection ($-u\ \partial T/\partial x$) along with its component parts, the zonal temperature gradient ($\partial T/\partial x$) and the zonal wind (u). In May, the zonal term of temperature advection is small near Okinawa (Fig. 3.10a) because the local zonal temperature gradient is small (Fig. 3.10b). The zonal term of temperature advection around Okinawa grows during early June due to the persistence of moderate zonal winds in the presence of an increasing zonal temperature gradient (Fig. 3.10c). The zonal wind speed weakens after mid-June, and the region of strong zonal temperature advection shifts northward from Okinawa. Zonal temperature advection near Okinawa approaches zero at this stage.

Figure 3.11 shows the meridional term of temperature advection ($-v\ \partial T/\partial y$) and its component parts. The meridional term of temperature advection is large near Okinawa in mid-May (Fig. 3.11a) because the meridional temperature gradient is strong (Fig. 3.11b) and meridional winds are moderate and southerly (Fig. 3.11c). The meridional temperature gradient weakens after mid-May, and the meridional term of temperature advection remains small throughout June even as the meridional wind strengthens. The occurrence of the baiu front over Okinawa in mid-May is due mainly to southerly winds in the presence of a north–south temperature contrast, while the baiu front over Okinawa in early and mid-June is due mainly to westerly winds in the presence of an east–west temperature contrast.

The warm advection mechanism proposed by Sampe and Xie (2010), in which westerly winds and an east–west temperature contrast combine to enhance warm advection and trigger strong upward motion through convective feedback, can be used to explain the Okinawa baiu during June. This mechanism cannot explain the Okinawa

baiu during May, as the warm advection during May is primarily due to the combination of southerly winds and a north–south temperature contrast.

3.4 Convective instability

In this section, we investigate the evolution of convective stability and its relationship with the Okinawa baiu. We calculate convective instability as the difference in moist static energy between 925 hPa and 600 hPa. Large positive values indicate an unstable atmosphere. Convective instability is greater in the southern part of the Okinawa region, where SSTs are relatively warm, than in the northern part, where SSTs are relatively cool.

The Okinawa region is weakly unstable to convection during May, when convective activity over the East China Sea is weak (Figs 3.12a–c and 3.4a–f). Weak convective instability over the Okinawa region during mid-May becomes weakly stable conditions during late May (Fig. 3.12c). The region of convective instability then extends northward to approximately 35°N during June (Fig. 3.12d–f). This northward extension of the unstable region is associated with a northward extension of relatively warm SSTs. Convective instability remains high in the Okinawa region into late June, following the northward withdrawal of the Okinawa baiu. The evolution of convective instability is therefore unable to explain the full evolution of the Okinawa baiu season; by contrast, horizontal temperature advection offers a more consistent explanation from onset to withdrawal. Transient weather disturbances may also play a role.

3.5 Role of transient weather disturbances

The behavior of the Okinawa baiu during May cannot be explained solely by warm advection. One factor that remains to be explored is the possible contribution of typhoons. Typhoons develop in the more uniform tropical atmosphere and are not related to large-scale warm advection; therefore the mechanism proposed by Sampe and Xie (2010) for baiu formation and maintenance does not apply. Typhoons sometimes approach Okinawa and make landfall in Okinawa during the May–June period (Table 3.1). We select days during which no typhoons approached to within 300 km of Okinawa for further study from meteorological chart of each years. The mid-May peak in mean precipitation amount over these days without a typhoon is 9 mm day^{-1}, approximately 20% decrease of the 10-year mean; however, the peak in mean precipitation amount during June changes little relative to the 10-year mean (Fig. 3.13). This result suggests that the 10-year mean of mid-May precipitation is marginally enhanced by typhoon activity, which brings convective rainfall but is not related to the large-scale frontal system. Typhoon is one of transient disturbances. In general, the evolution of transient eddy activity corresponds well to the evolution of the Okinawa baiu.

In this section, we examine the role of transient disturbances such as synoptic-scale low pressure systems and typhoons in the evolution of the Okinawa baiu. Figure 3.14 shows transient eddy activity as measured by the standard deviations of selected meteorological variables during three distinct phases of Okinawa baiu development (initial peak in mid-May, short break in late May, and second peak in June). We apply a high-pass filter with a cutoff period of 7 days.

Active disturbances in the meridional wind occur along the westerly jet stream

during all three phases of baiu development (Fig. 3.14a–c). The region of active disturbances shifts southward toward Kyushu (30°–35°N, 130°E) during the short break in the Okinawa baiu in late May (Fig. 3.14b), while it is situated over Okinawa during June (Fig. 3.14c). Transient variability in 500-hPa temperature is large northward of 30°N (Fig. 3.14d–f), and also shifts southward during the late May break in the Okinawa baiu (Fig. 3.14e). Fluctuations in low-level specific humidity in precipitation areas are large during the Okinawa baiu (Figs 3.4d-e, h and 3.14g–i). As with meridional wind disturbances (Fig. 3.14b) and temperature variability (Fig. 3.14), these fluctuations in specific humidity shift southward during the break period in late May (Fig. 3.14). All three variables indicate that transient weather activity decreases in the Okinawa region during late June, when the Okinawa baiu withdraws (not shown). The seasonal evolution of precipitation in the Okinawa region is generally consistent with that of transient weather disturbances as Sampe and Xie (2010). Relative to mid-June, the mid-May Okinawa baiu is more heavily affected by transient weather disturbances. This result is consistent with the intermittent nature of baiu precipitation events during May (Ishigaki 1982).

Table 3.1 Number of typhoon approaches to within 300 km of Okinawa region for 10-years from 1997 to 2006.

year	Jan	Feb	Mar	Apr	May	Jun	Jul	Aug	Sep	Oct	Nov	Dec
1997					1	2	1	3	1	1		
1998								2	2	1		
1999							2	3	1		1	
2000					1		2	3	2	1	1	
2001					1		1	1	2	1		
2002						1	5	1	1			
2003				1	1	2		2	2		1	
2004					1	2	1	4	3	3		1
2005						1	1	2	3	2		
2006							3	2	1			
Number				1	5	8	16	23	18	9	3	1

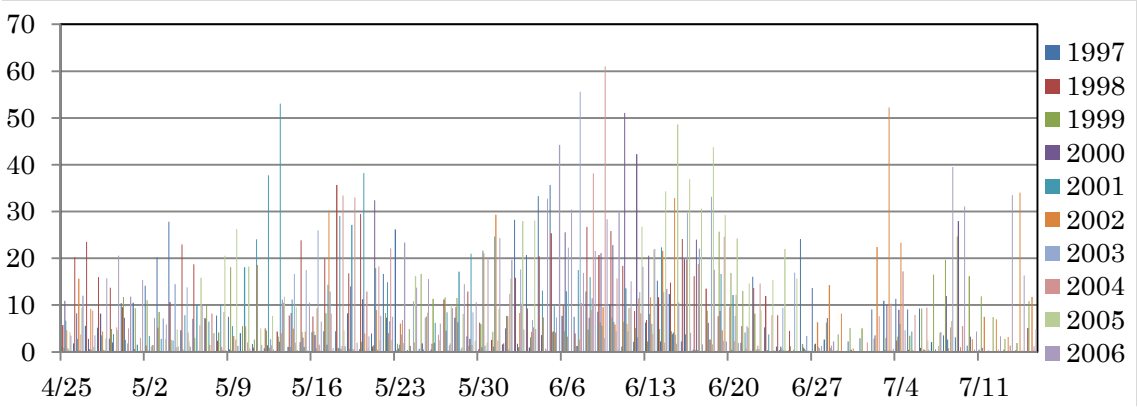

Figure 3.1: Time series of daily precipitation in the Okinawa region for each year (mm day^{-1}) from 25 April to 15 July.

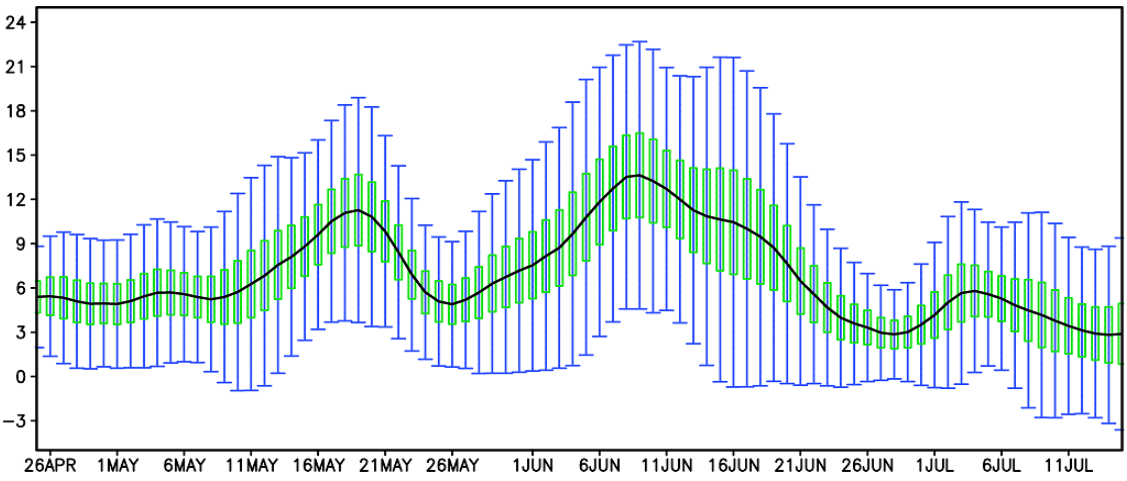

Figure 3.2: Time series of 10-year mean precipitation in the Okinawa region from 25 April to 15 July. The black solid line is derived by twice applying a 5-day running mean to smooth the GPCP data (unit of mm day^{-1}). The blue bar shows the standard deviation and the green bar shows the standard error.

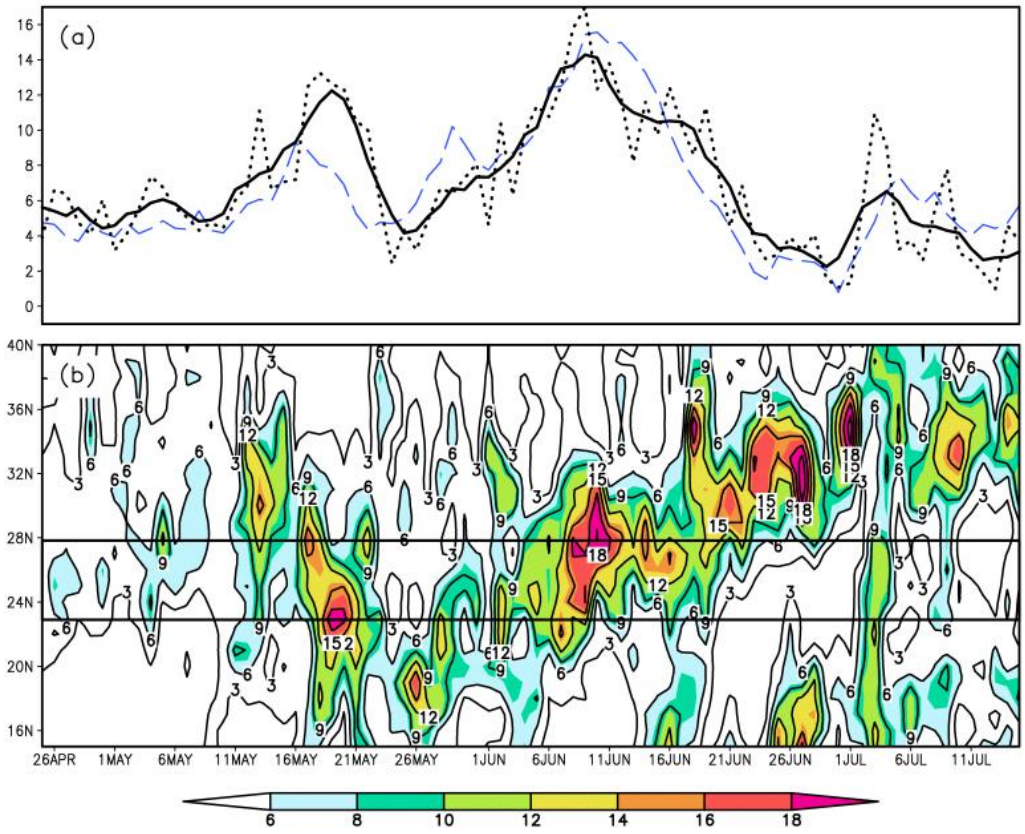

Figure 3.3: Temporal evolution of precipitation in the Okinawa region. (a) Time series of precipitation (mm day^{-1}) over the Okinawa region (23°–28°N and 123°–129°E) from 25 April to 15 July based on 10-year climatologies from GPCP (dotted line) and APHRODITE (blue dashed line). The black solid line is derived by twice applying a five-day running mean to smooth the GPCP data. (b) Time–latitude variation of GPCP precipitation averaged over the longitudinal range 123°–129°E with a contour interval of 3 mm day^{-1}. The black horizontal lines indicate the boundaries of the Okinawa region.

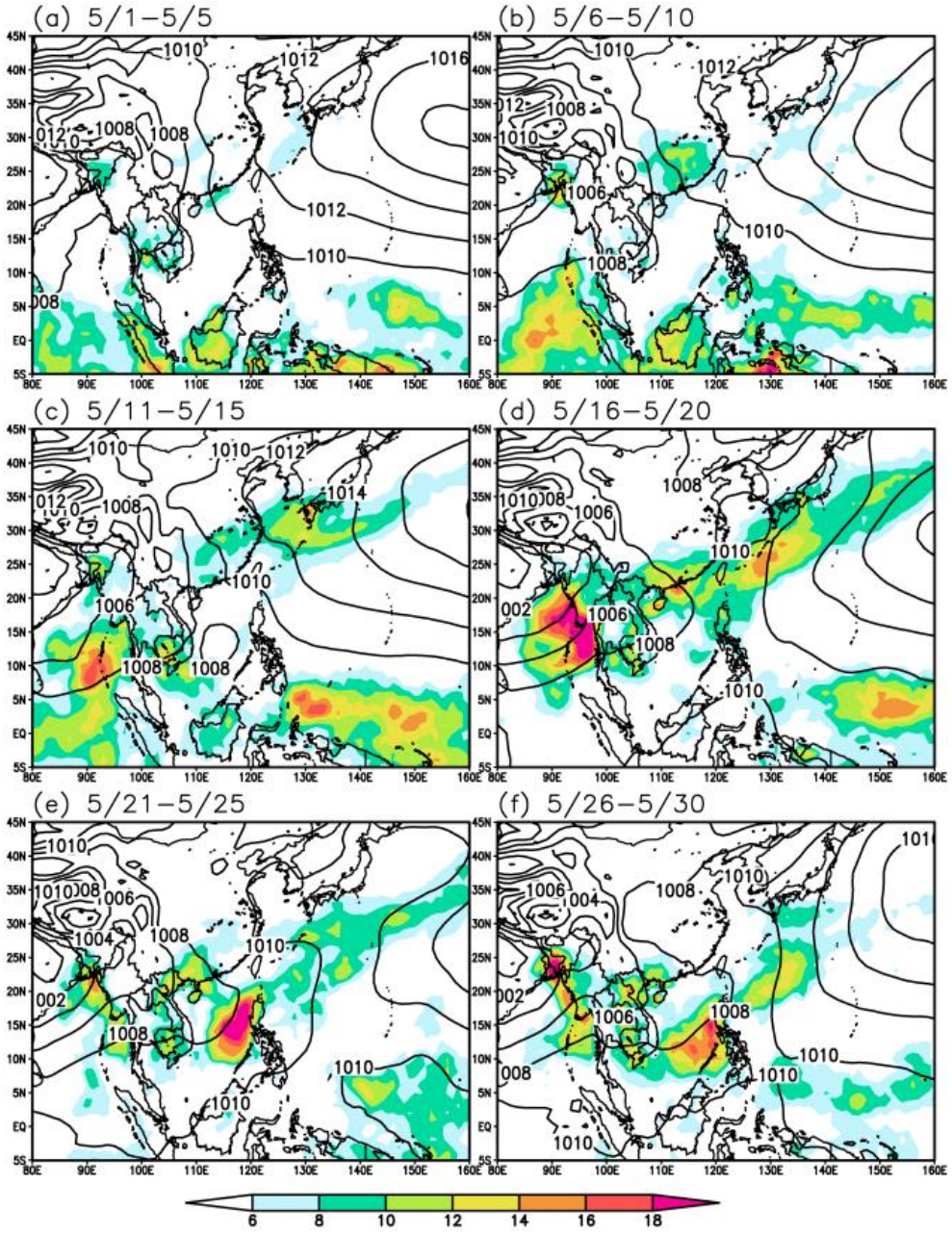

Figure 3.4: Average precipitation (color shading; mm day^{-1}) and sea level pressure (SLP) (solid contours; hPa) for individual pentads during the Okinawa baiu: (a) 1–5 May, (b) 6–10 May, (c) 11–15 May, (d) 16–20 May, (e) 21–25 May, and (f) 26–30 May.

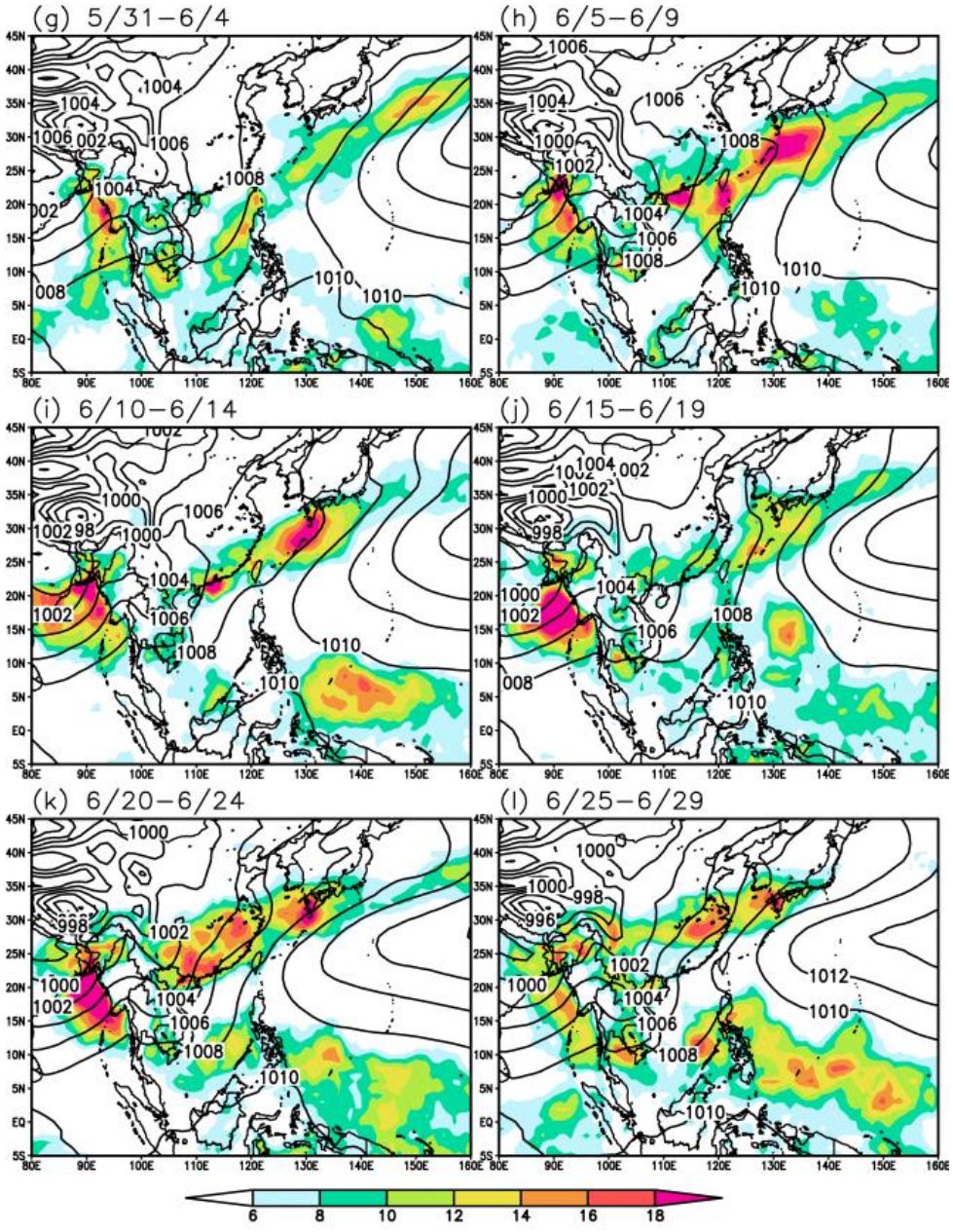

Figure 3.4: (Continued): (g) 31 May–4 June, (h) 5–9 June, (i) 10–14 June, (j) 15–19 June, (k) 20–24 June, and (l) 25–29 June.

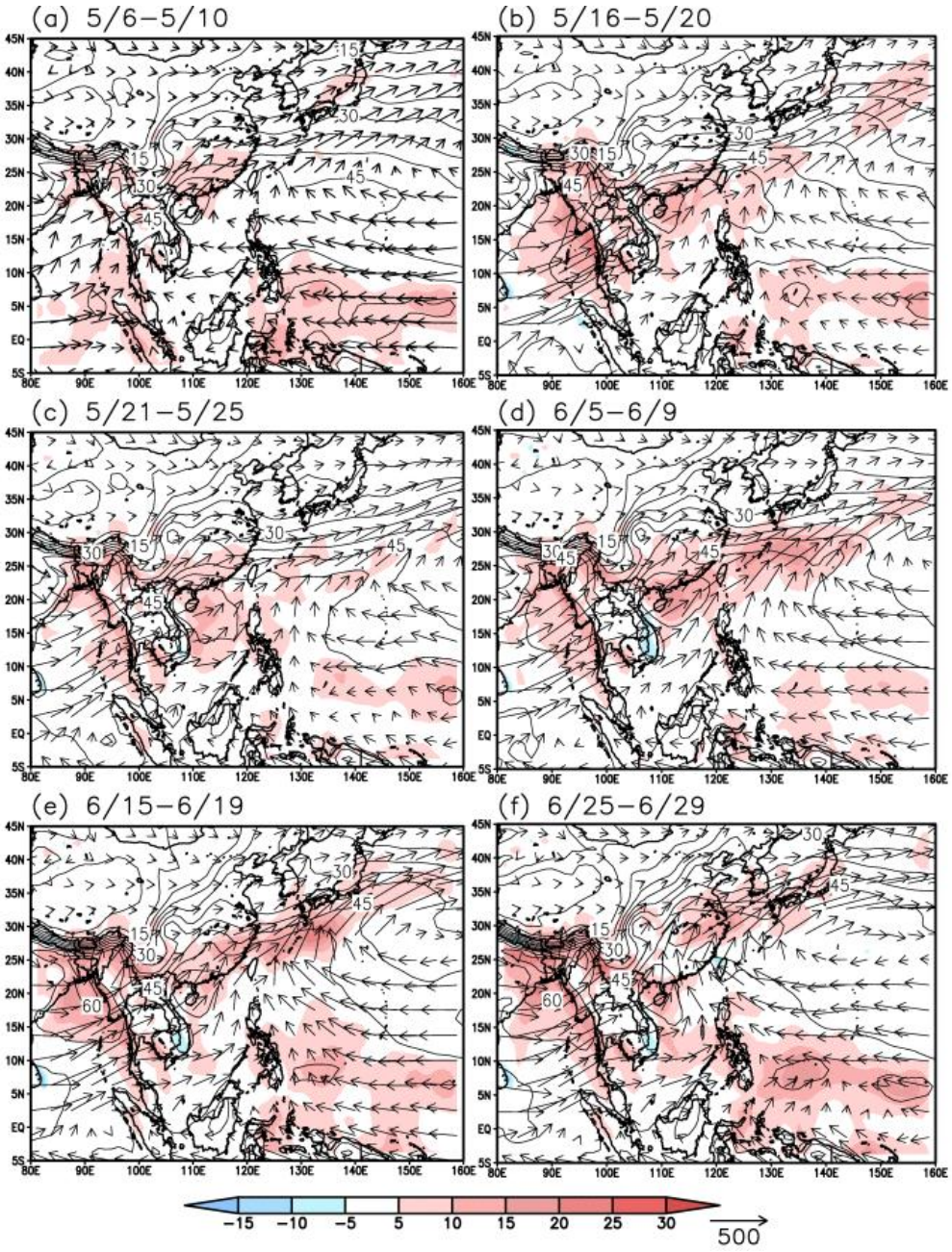

Figure 3.5: Moisture flux (arrows; kg m^{-1} day^{-1}), moisture flux convergence (shading; kg m^{-2} day^{-1}), and precipitable water (solid contours; mm) for selected pentads during the Okinawa baiu: (a) 6–10 May, (b) 16–20 May, (c) 21–25 May, (d) 5–9 June, (e) 15–19 June, and (f) 25–29 June. Moisture fluxes are vertically integrated from the surface to 200 hPa.

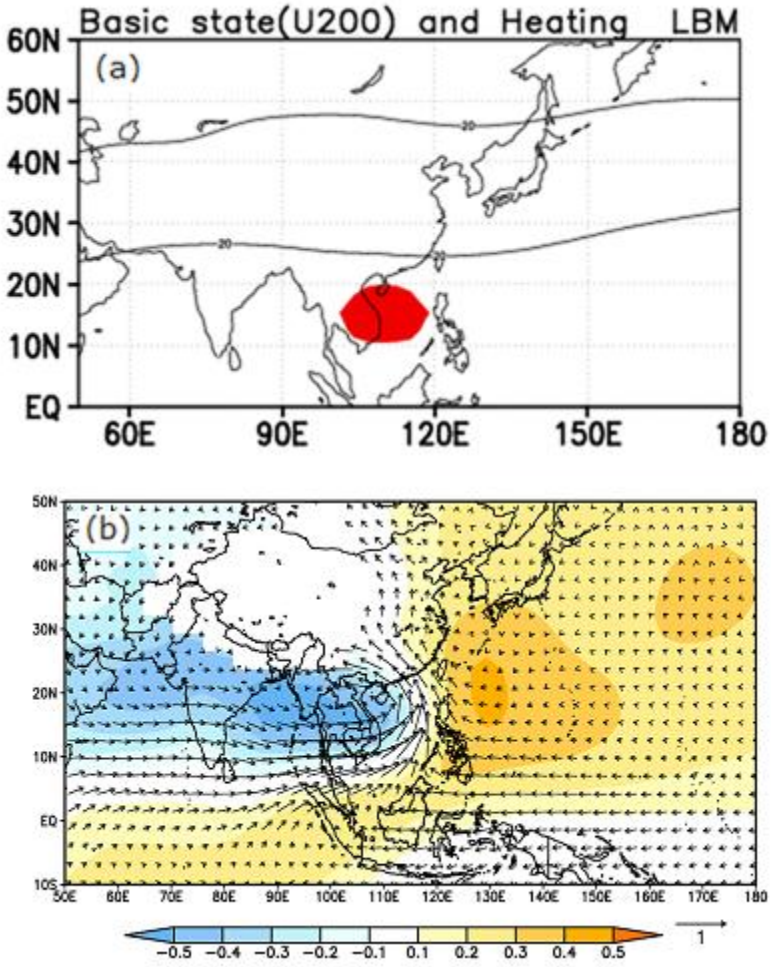

Figure 3.6: LBM response to idealized heating centered at 15°N, 110°E in May. (a) Heat source and 200-hPa zonal wind (unit: m s^{-1}). (b) 850-hPa stream function (unit: 10^6 m^2 s^{-1}) an wind (arrows: m s^{-1}).

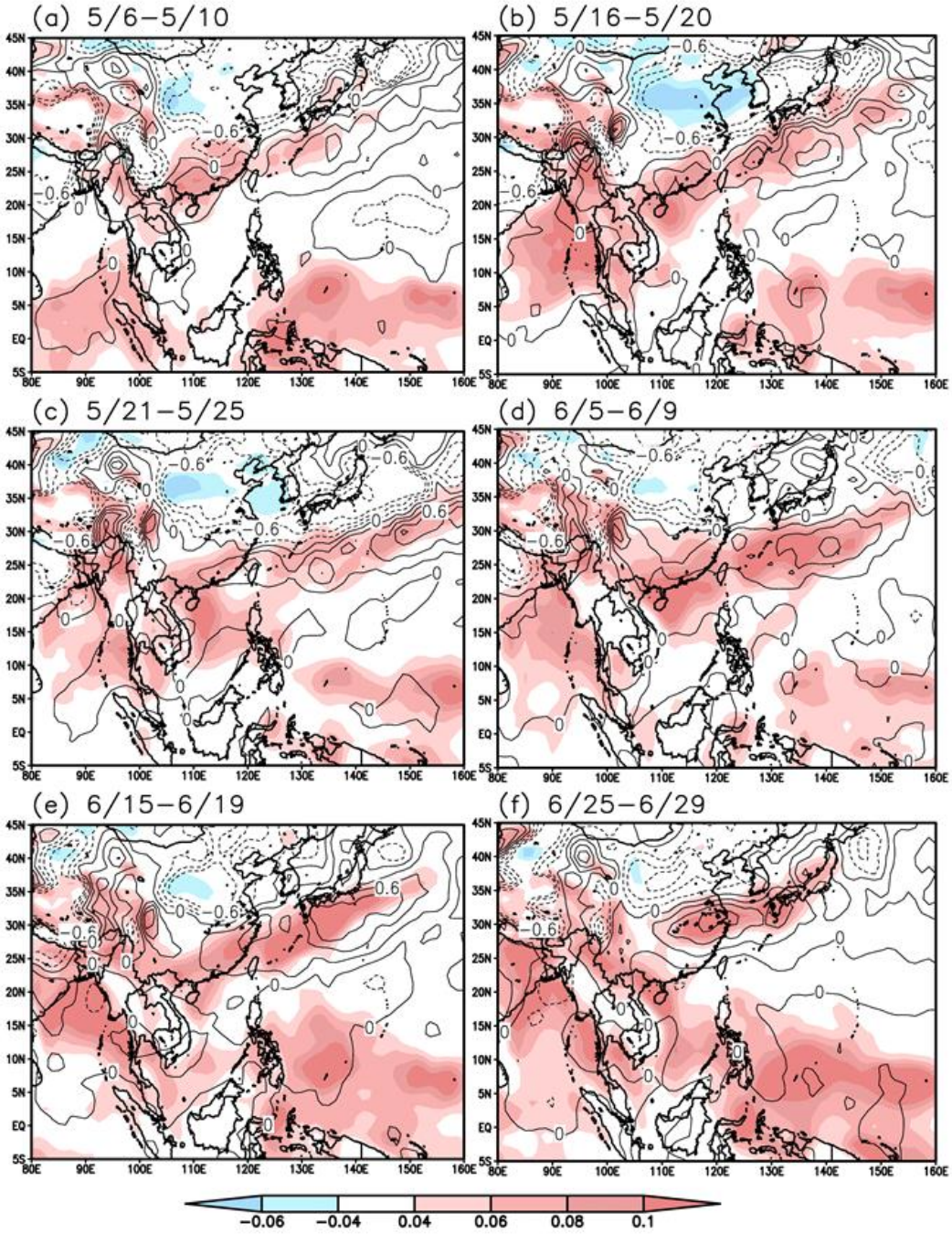

Figure 3.7: Horizontal temperature advection (solid contours; contour interval 0.2 K day^{-1}) and upward vertical pressure velocity ($-\omega$) (shading; Pa s^{-1}) at 500 hPa for selected pentads during the Okinawa baiu: (a) 6–10 May, (b) 16–20 May, (c) 21–25 May, (d) 5–9 June, (e) 15–19 June, and (f) 25–29 June. Contours of horizontal temperature advection less than –0.6 K day^{-1} are omitted.

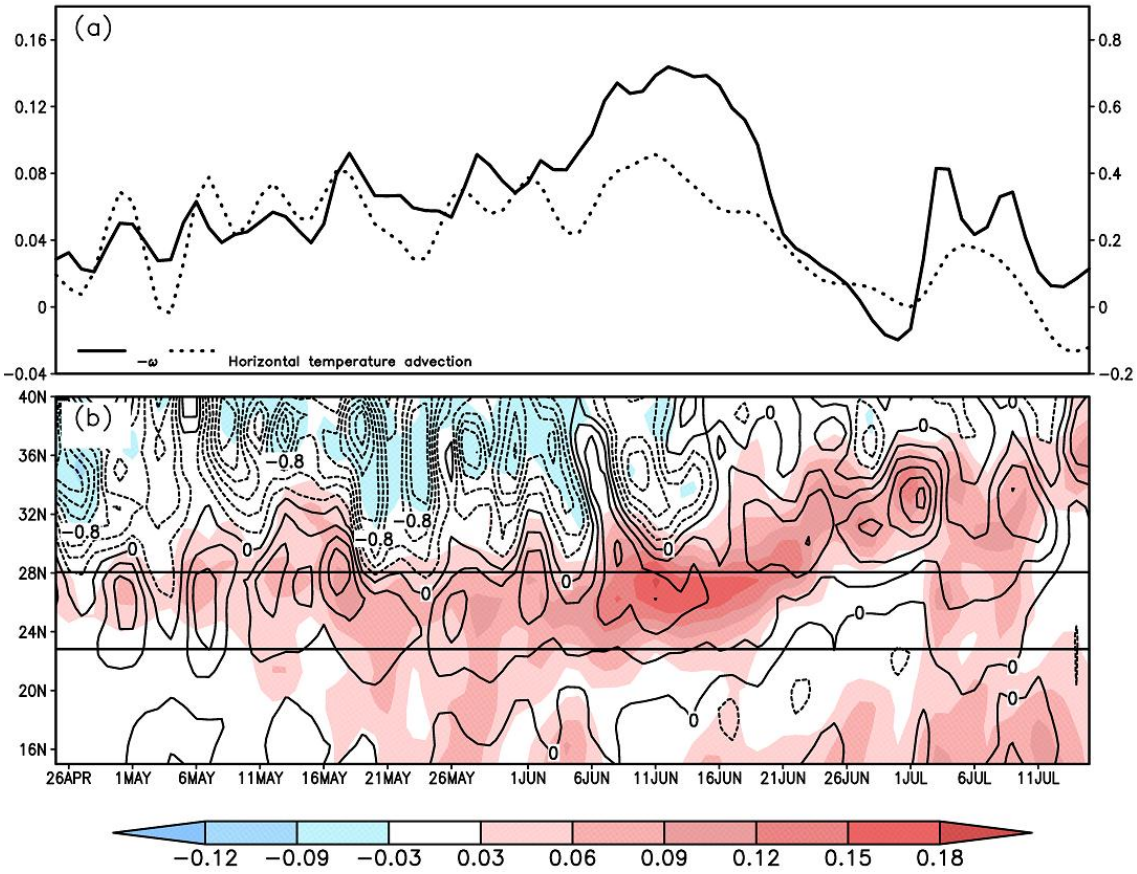

Figure 3.8: (a) Time series of upward vertical pressure velocity ($-\omega$) at 500 hPa (solid line; left axis; Pa s^{-1}) and horizontal temperature advection at 500 hPa (dotted line; right axis; K day^{-1}) averaged over the Okinawa region. Three-day running means are applied for smoothing. (b) Time–latitude plots of –ω (shading) and 500-hPa horizontal temperature advection (solid contours; contour interval 0.2 K day^{-1}) averaged over the longitudinal range 123°–129°E. Positive values denote upward vertical velocity and warm advection; negative values denote downward vertical velocity and cold advection. The black horizontal lines indicate the boundaries of the Okinawa region.

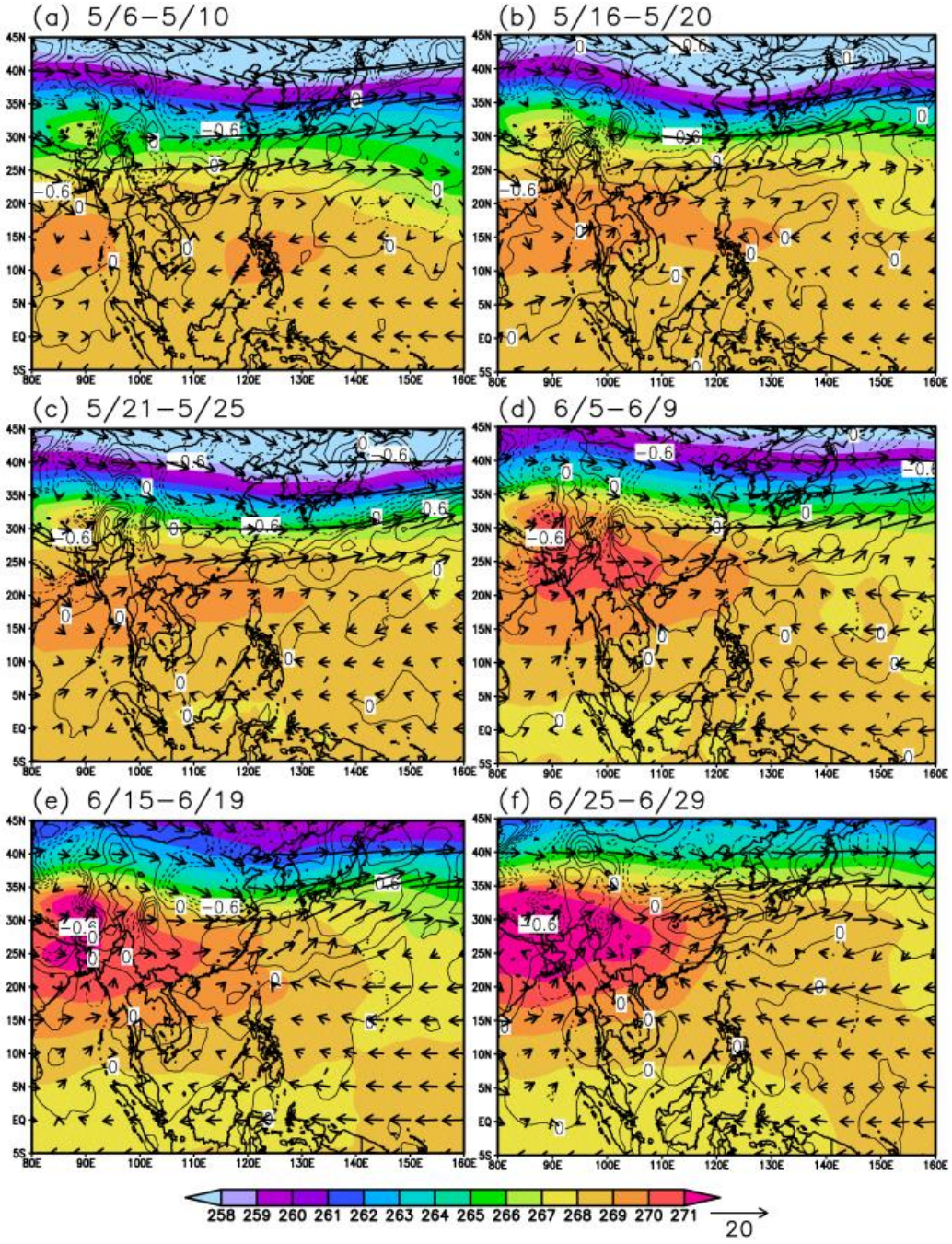

Figure 3.9: Mean horizontal wind (arrows; m s^{-1}), horizontal temperature advection (solid contours; 0.2 K day^{-1}), and temperature (color shading; K) at 500 hPa for selected pentads during the Okinawa baiu: (a) 6–10 May, (b) 16–20 May, (c) 21–25 May, (d) 5–9 June, (e) 15–19 June, and (f) 25–29 June.

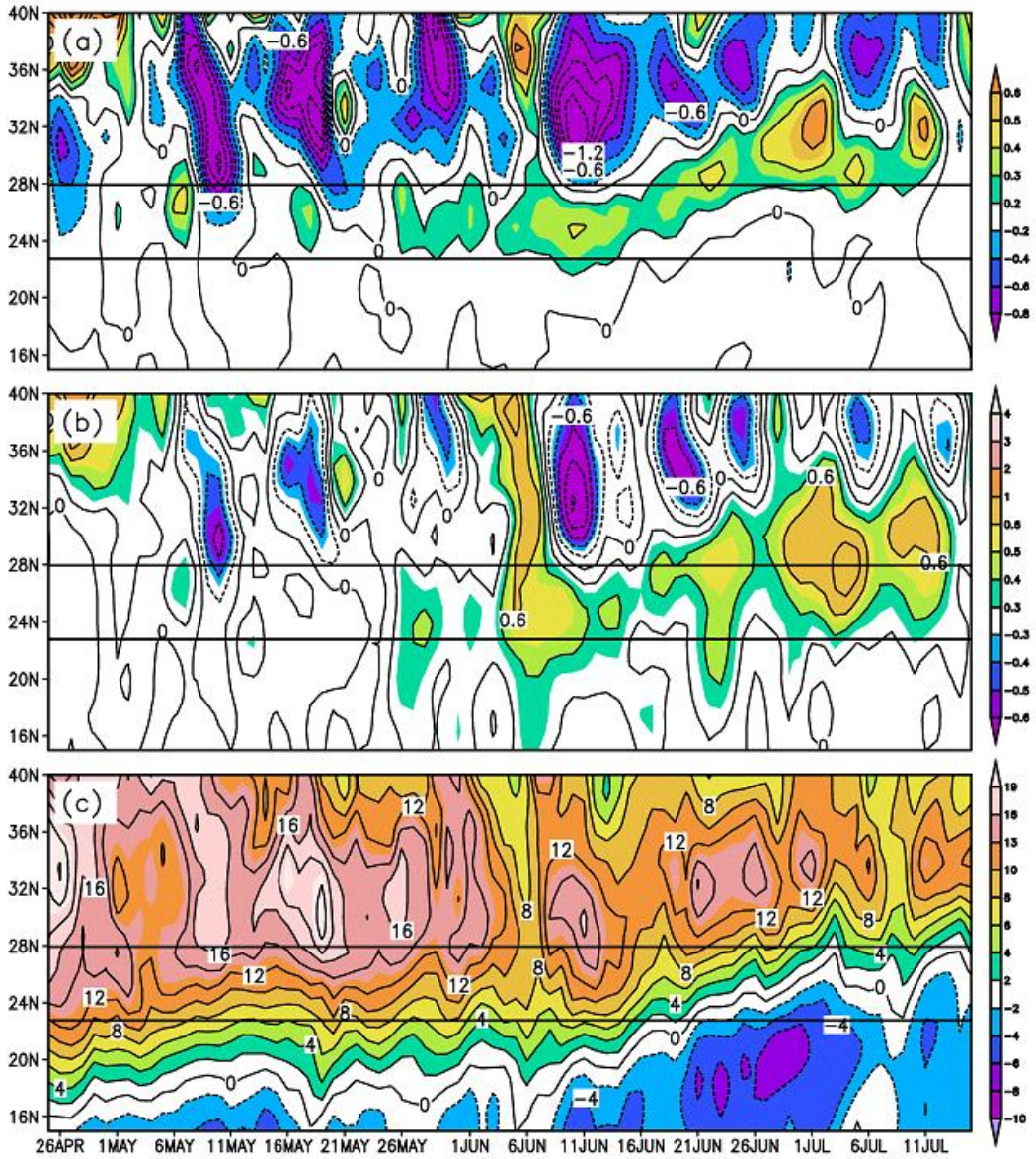

Figure 3.10: Time–latitude plots of (a) zonal horizontal temperature advection (contour interval 0.2 K day^{-1}), (b) zonal temperature gradient (contour interval 0.2 × 10^{-5} K m^{-1}), and (c) zonal wind (contour interval 2 m s^{-1}). All panels show values at 500 hPa averaged over the longitudinal band 123°–129°E. Three-day running means are applied for smoothing. The black horizontal lines indicate the boundaries of the Okinawa region.

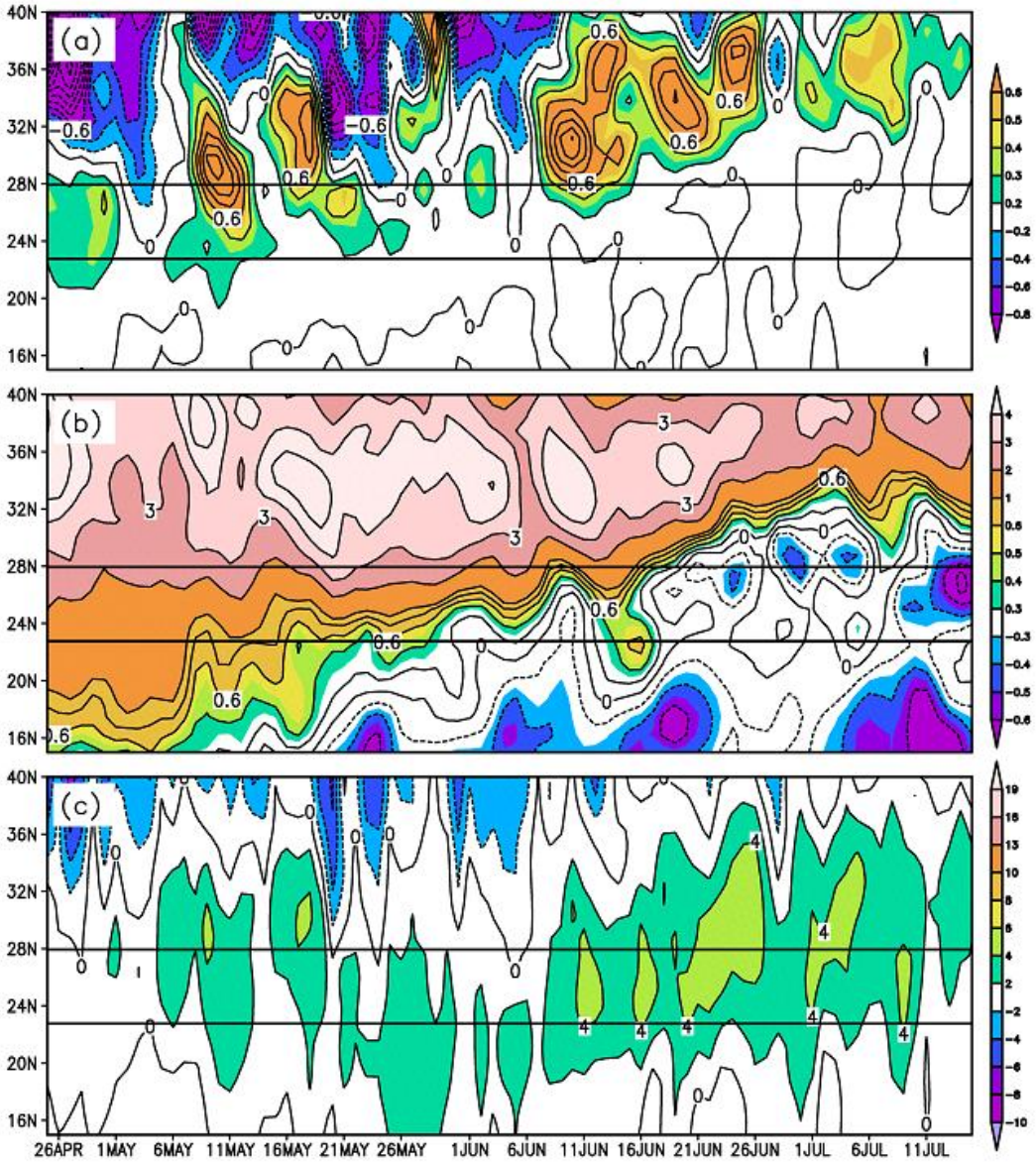

Figure 3.11: As in Fig. 3.9, but for (a) meridional horizontal temperature advection (contour interval 0.2 K day^{-1}), (b) meridional temperature gradient (contour interval 0.2 $\times$ 10^{-5} K m^{-1}), and (c) meridional wind (contour interval 2 m s^{-1}).

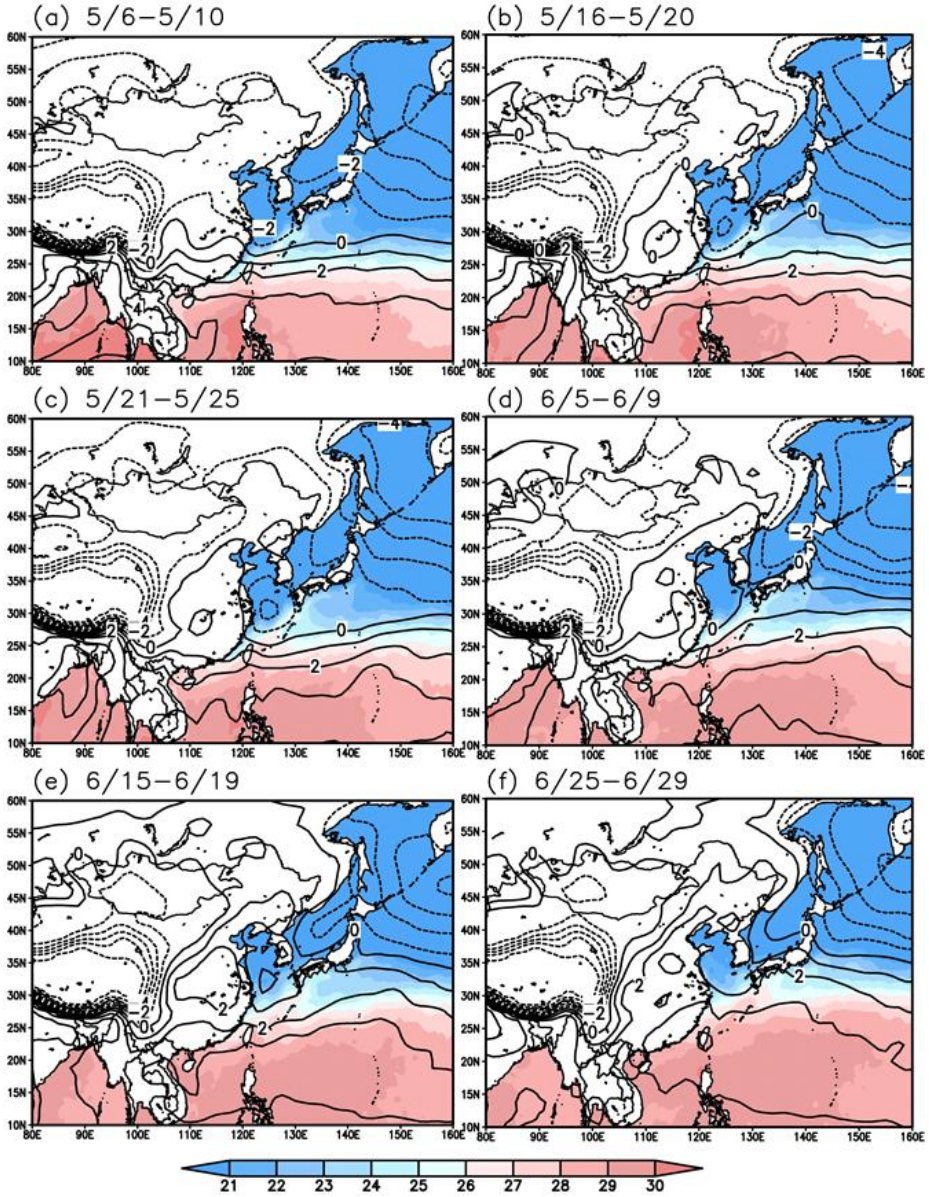

Figure 3.12: Vertical gradients of moist static energy between 925 and 600 hPa divided by the specific heat at constant pressure (solid lines; contour interval 1 K (100 hPa)$^{-1}$; large positive values indicate an unstable atmosphere) and sea surface temperature (SST; color shading, ˚C) for selected pentads during the Okinawa baiu: (a) 6–10 May, (b) 16–20 May, (c) 21–25 May, (d) 5–9 June, (e) 15–19 June, and (f) 25–29 June.

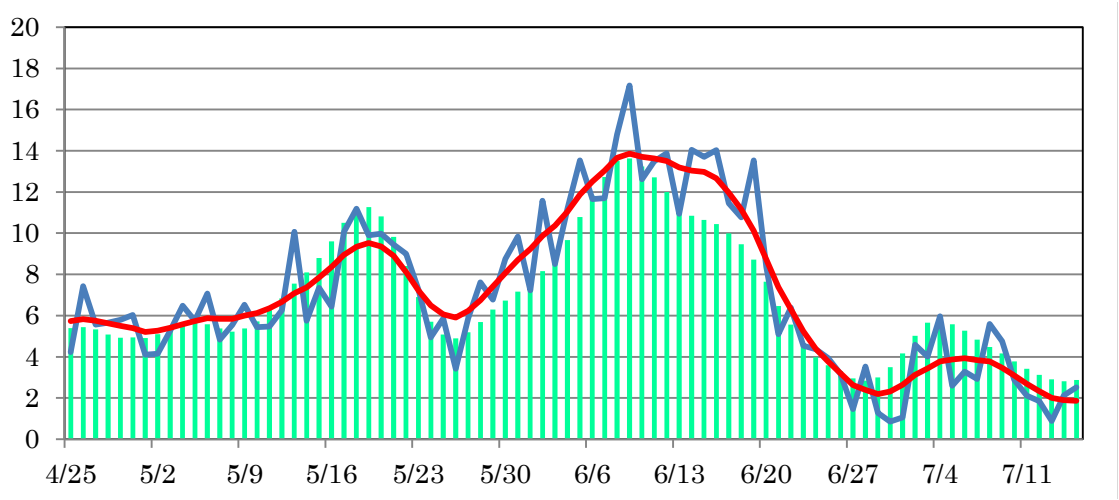

Figure 3.13: Temporal evolution of precipitation in the Okinawa region from 25 April to 15 July based on 10-year climatologies. The blue line is raw time-series of precipitation excluding a typhoon and the red line is derived by twice applying a 5-day running mean to smooth this data. The green bar is time-series of smoothed 10-year climatologies.

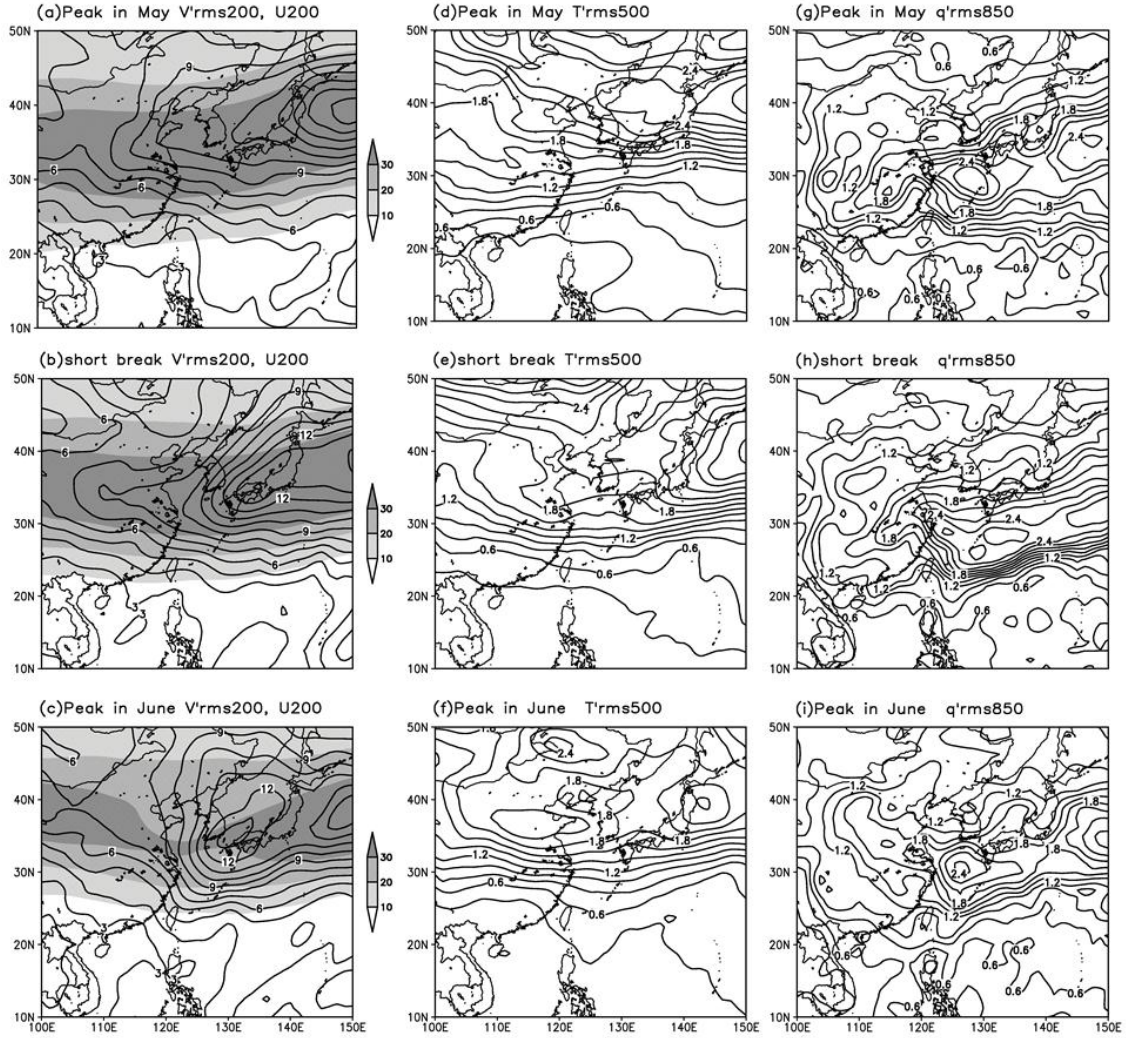

Figure 3.14: Mean rms (root mean square) of high-pass-filtered (a)–(c) 200-hPa meridional wind (contours; contour interval 1 m s^{-1}) and 200-hPa zonal wind speed (shading; m s^{-1}), (d)–(f) 500-hPa temperature (contours; contour interval 0.2 K), and (g)–(i) 850-hPa specific humidity (contours; contour interval 0.2×10^{-3} kg kg^{-1}) for selected pentads during the Okinawa baiu: (a), (d), (g) 16–20 May, (b), (e), (h) 21–25 May, and (c), (f), (i) 5–9 June.

Chapter 4

Interannual variability

In this chapter, the interannual variability of the Okinawa baiu and the associated large-scale features are examined. As shown in the previous chapters, the large-scale meteorological characteristics of the Okinawa baiu in May and June are different. Thus we investigate the interannual variability in May and that in June separately. To improve the statistical significance, we use monthly data for 30 years from 1979 to 2008.

4.1 Interannual variability of precipitation during the Okinawa baiu

The 30-year time-series of monthly precipitation averaged over the Okinawa region in May and June are shown in Fig.4.1a. The correlation between two months is 0.185 and is not statistically significant. Thus the precipitation amount in May and that in June are independent. Horizontal distributions of the mean precipitation together with the standard deviation are shown in Fig.4.1b and 4.1c for May and June, respectively. The variability of precipitation in May is large over south of Okinawa region (Fig. 4.1b), while that in June almost corresponds to mean precipitation fields (Fig. 4.1c).

The rainy season in East Asia is generally characterized by two active rainfall periods (Chen et al. 2004). The standard deviation of precipitation during baiu period around Okinawa region is about 3.0 mm day^{-1}, while that in typhoon season (August

and September) is about 3.5 mm day^{-1}. The 30-year (1979-2008) data shows that the number of typhoon approaches to Okinawa in typhoon season is three times larger than that in baiu season. Precipitation variability during baiu is large next to typhoon seasons. The baiu rainband is situated around Okinawa and displays a large interannual variability both in May and June. In the following, correlation /regression analysis of meteorological fields against the precipitation over the Okinawa region is made separately for May and June to examine the relationship between the precipitation around Okinawa region and environmental fields.

4.2 May

Firstly, correlation of precipitation itself with the Okinawa precipitation is examined. In May, the region of positive correlation of precipitation with Okinawa precipitation extends northeastward from the South China Sea (SCS) to the south of Japan (Fig. 4.2a). The positive correlation region generally extends along the baiu rainband (see Fig. 4.1b). Weak negative correlations are seen over Yellow Sea and northwestern subtropical Pacific (10°N, 140°-160°E). The convergence of moisture flux shows positive significant correlation in southeastern part of the Okinawa region and negative correlations are found to the north and southeast of the Okinawa region where those in precipitation are negative (Fig. 4.2b).

Figure 4.3 shows that the relationship between precipitation of Okinawa region and temperature advection at 500 hPa. The correlation in May is small around Okinawa region, but it is marginally significant. When the temperature advection is divided into meridional and zonal terms, both terms are not significant (Fig. 4.4). Instead, negative

correlation is seen to the north of Okinawa, especially in the zonal term, which indicates the cold advection to the north of Okinawa is associated with heavy rainfall over the Okinawa region in May (Fig.4.3 and Fig.4.4).

Correlations map for temperature (shading) and wind (arrows) at 500 hPa and 850 hPa are shown in Fig. 4.5. The temperature at 850 hPa show positive significant correlation over the seas off the east coast of the Philippines and also significant southerly winds are seen over the same region (Fig. 4.5b). Over Okinawa, cyclonic circulation is positively correlated with the Okinawa precipitation. This result shows that it is favorable for active Okinawa baiu that the warm and moist air is supplied into baiu rainband around Okinawa region by southerly wind at the lower troposphere. In the middle troposphere (500 hPa), the significant positive correlation exists south of China, Taiwan and western part of Okinawa, while significant negative coefficient exists over northern China (Fig. 4.5a). Again the southerly wind is significant around Okinawa and to the south of Okinawa as is the case with the lower troposphere.

We also investigate the relationship with sea surface temperature (SST). The significant positive correlation is not found around Okinawa region but marginally positive signal is found near southern Philippines (Fig. 4.6b). The change of SST is slow compared with air temperature and thus we computed the correlation with the SST in the previous month, i.e., April (Fig. 4.6a). The significant SST signals are seen around Philippines and no signals around Okinawa region in one month prior (Fig. 4.6a). Even if the global correlation map is examined, other signal is not found (Fig. 4.7).

4.4 June

The region of positive correlation of precipitation with Okinawa precipitation

extends from the Southern China to the south of Japan in June (Fig. 4.9a). The convergence of moisture flux shows a significant positive correlation over the same region (Fig. 4.9b). The negative correlations are found to the north of positive region (from central China to western Japan) and around Philippines (Fig 4.9b).

The correlation between the precipitation in June and temperature advection at 500 hPa is large around Okinawa region (Fig. 4.10), compared with the result of May (Section 4.2.1). This result suggests that the relationship between baiu rainband and temperature advection at 500 hPa proposed by Sampe and Xie (2010) is applicable also to interannual varriability. Kosaka et al. (2011) also showed about this relationship by using a singular value decomposition (SVD) analysis. Also the relationship for each terms of temperature advection is large (Fig. 4.11). The positive correlation is seen over the Okinawa region and the western China in the zonal term and over the Japan islands in the meridional term, while negative correlation exists over Japan islands in the zonal term and around eastern China in the meridional term.

The temperature at 850 hPa shows positive significant correlations from the SCS and westward, and a significant cyclonic circulation centered at the northeast of Okinawa region is preferable for heavy precipitation over Okinawa (Fig. 4.12b). At 500 hPa, significant positive correlations of temperature exist over Indochina, while negative correlations exist from northern China to western Japan (Fig. 4.12a). The cyclonic circulation is also significant at 500 hPa but centered over East China Sea. This cyclonic flow brings warm air westward from Indochina in the middle troposphere and moist air from SCS (not shown) in the lower troposphere.

The relation with the simultaneous SST shows positive correlations in the SCS and Japan Sea (Fig. 4.13b). Unlike May, relationship between precipitation around Okinawa

region in June and SST in May has positive correlations over wide regions from East China Sea to the south of Japan (Fig. 4.13a). This result shows that if SST of this region in May is warm, the precipitation around Okinawa region is abundant in June. Globally, significant positive correlations are found at the equatorial eastern Pacific and this signal is seen since January (Fig. 4.14). It means the Okinawa baiu in June experiences abundant rainfall in the years when El Nino occurs in winter and continues into June. This relation of baiu precipitation with the El Nino – Southern Oscillation (ENSO) has been investigated by many works (Tanaka 1997; Wang et al. 2001; Huang et al. 2004; Tomita et al. 2004). Warm SST exists also in the tropical Indian Ocean from winter to summer (Fig. 4.14). Xie et al. (2009) proposed the following "Indian Ocean capacitor effect" to explain this lingering effect of ENSO: persistent warm anomalies in the tropical Indian Ocean SST after El Nino [Indian Ocean basin mode (IOBM)] excite a warm tropospheric Kelvin wave, which induces surface Ekman divergence over the tropical western North Pacific, triggers the Pacific-Japan (PJ) pattern, and eventually influences the meiyu-baiu rainband (Kosaka et al. 2011). However, the association with the PJ pattern is not found the Okinawa baiu rainfall in June, on the other hand, wave train from west Eurasia is seen (Fig. 4.15). The result of our analysis about SST suggests that the ENSO influences the precipitation of Okinawa baiu only in June, but it is not through the PJ pattern.

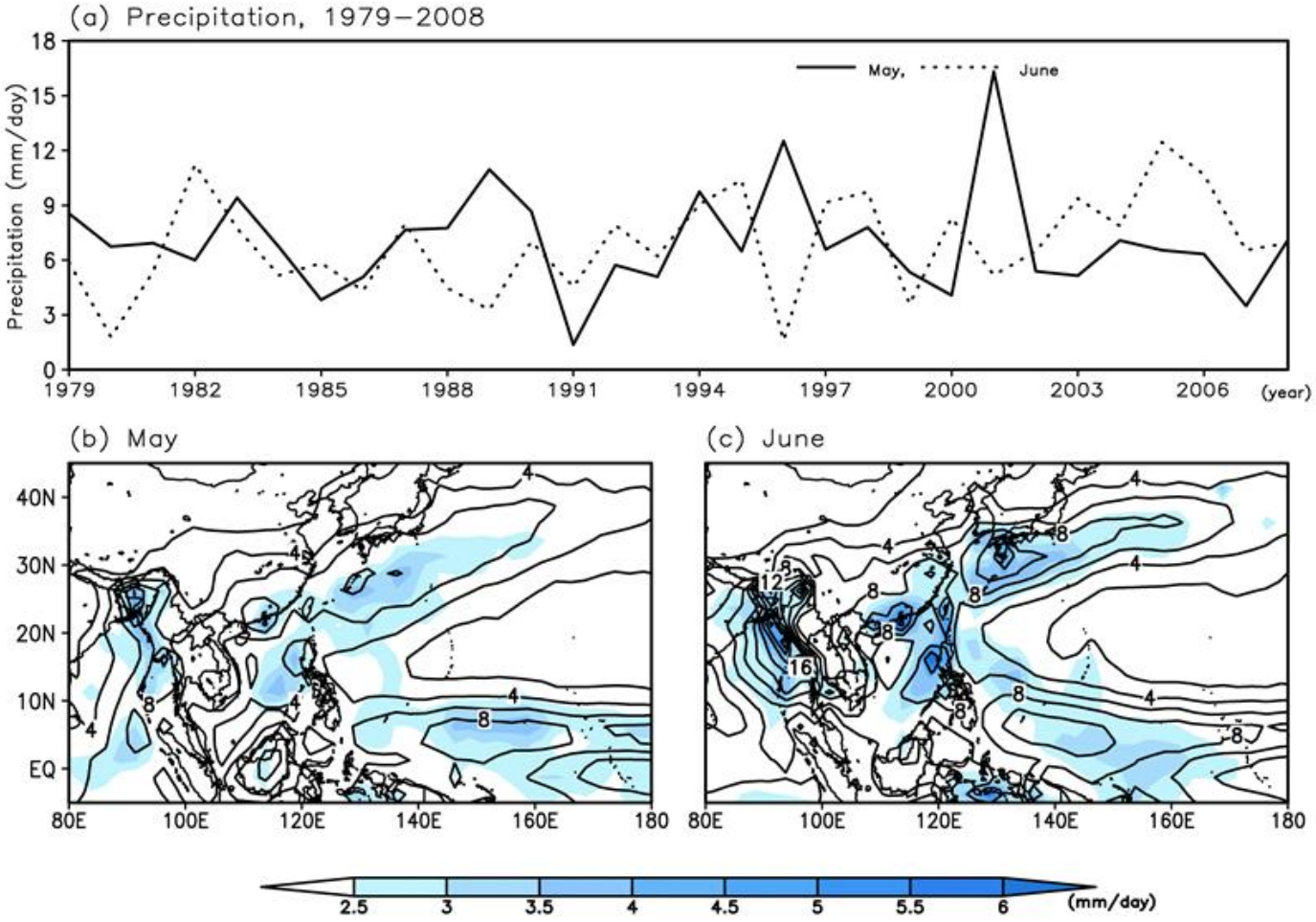

Figure 4.1: Inter-annual variation of precipitation in the Okinawa region for 30 years (1979-2008) and precipitation fields in May and June. (a) time-series of precipitation (solid line; May, dashed line; June, unit of mm day-1). GPCP precipitation (contour at every 2 mm day^{-1}) and standard deviation (shaded) for (b) May

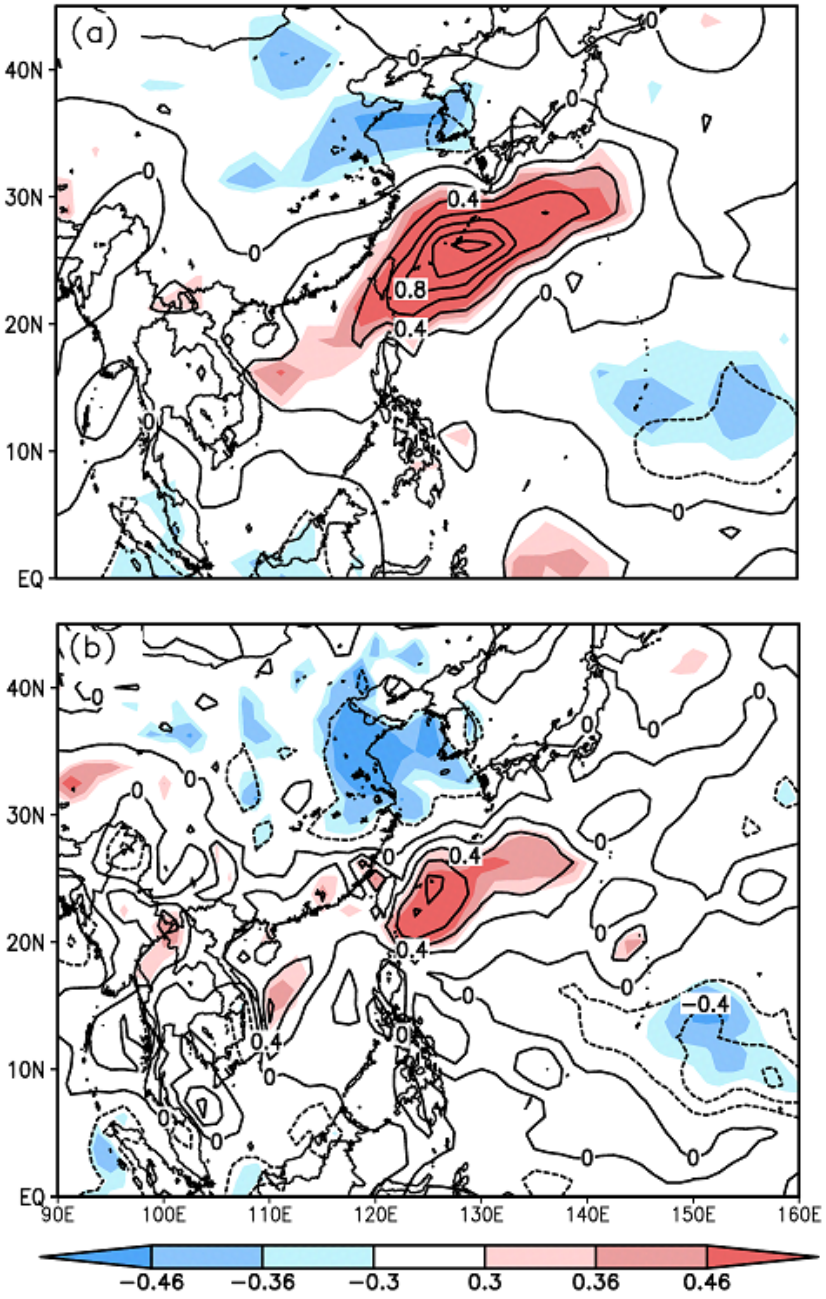

Figure 4.2: Correlation (shaded) and regression (contour) of interannual variations between precipitation of Okinawa region and (a) environmental precipitation, and (b) convergence (positive) / divergence (negative) of moisture flux in May. Contour interval is interval 0.2 mm day^{-1}. Shaded where correlation greater than 0.3 is significant at 90 % confidence level.

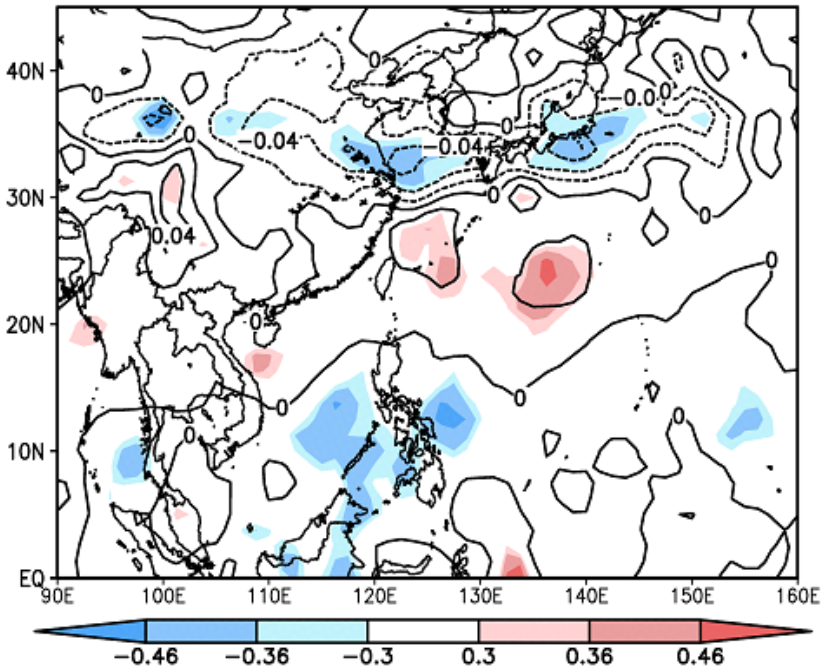

Figure 4.3: Same as Figure 4.2 but for with temperature advection at 500 hPa. Contour interval is 0.02 K day^{-1} with negative contours dashed. Shaded where correlation greater than 0.3 is significant at 90 % confidence level.

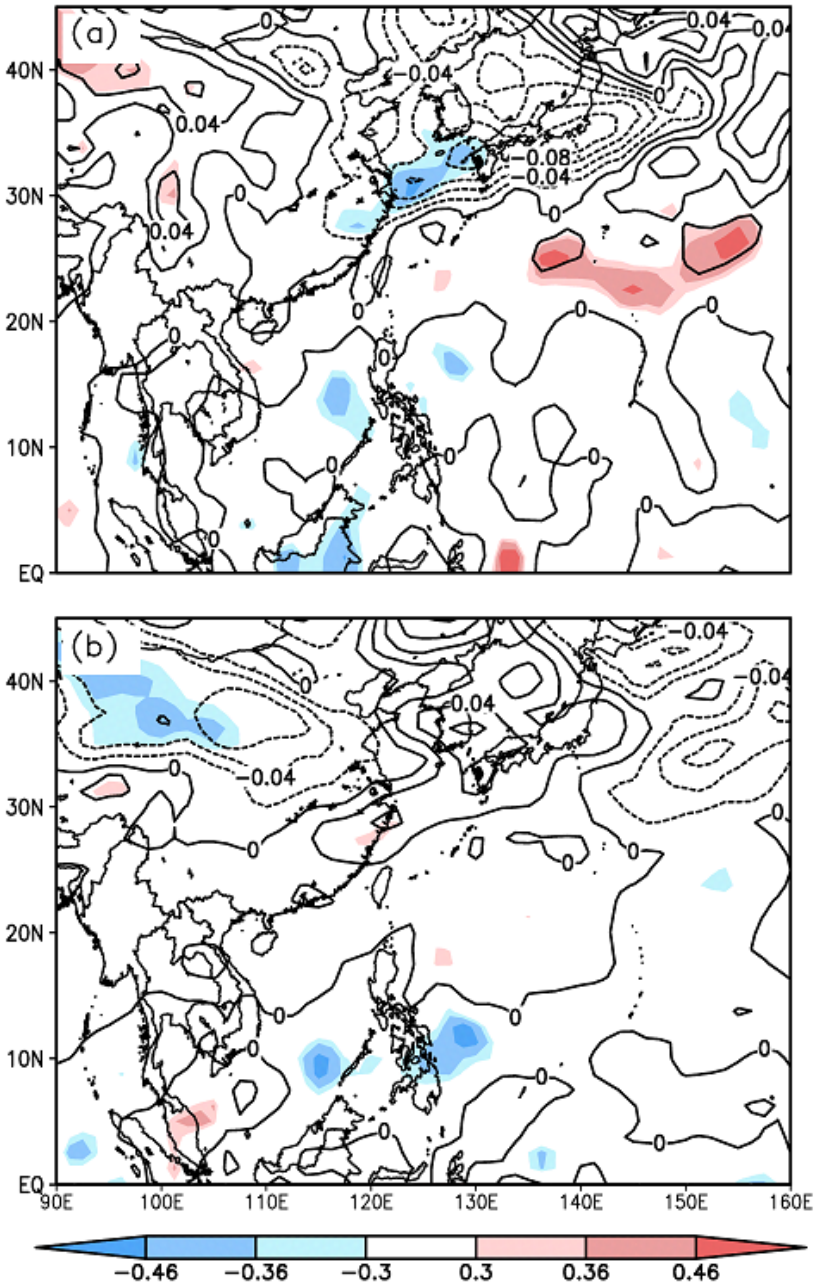

Figure 4.4: Same as Figure 4.3 but for with (a) zonal term, and (b) meridional term of 500-hPa temperature advection. Contour interval is 0.02 K day^{-1} with negative contours dashed. Shaded where correlation greater than 0.3 is significant at 90 % confidence level.

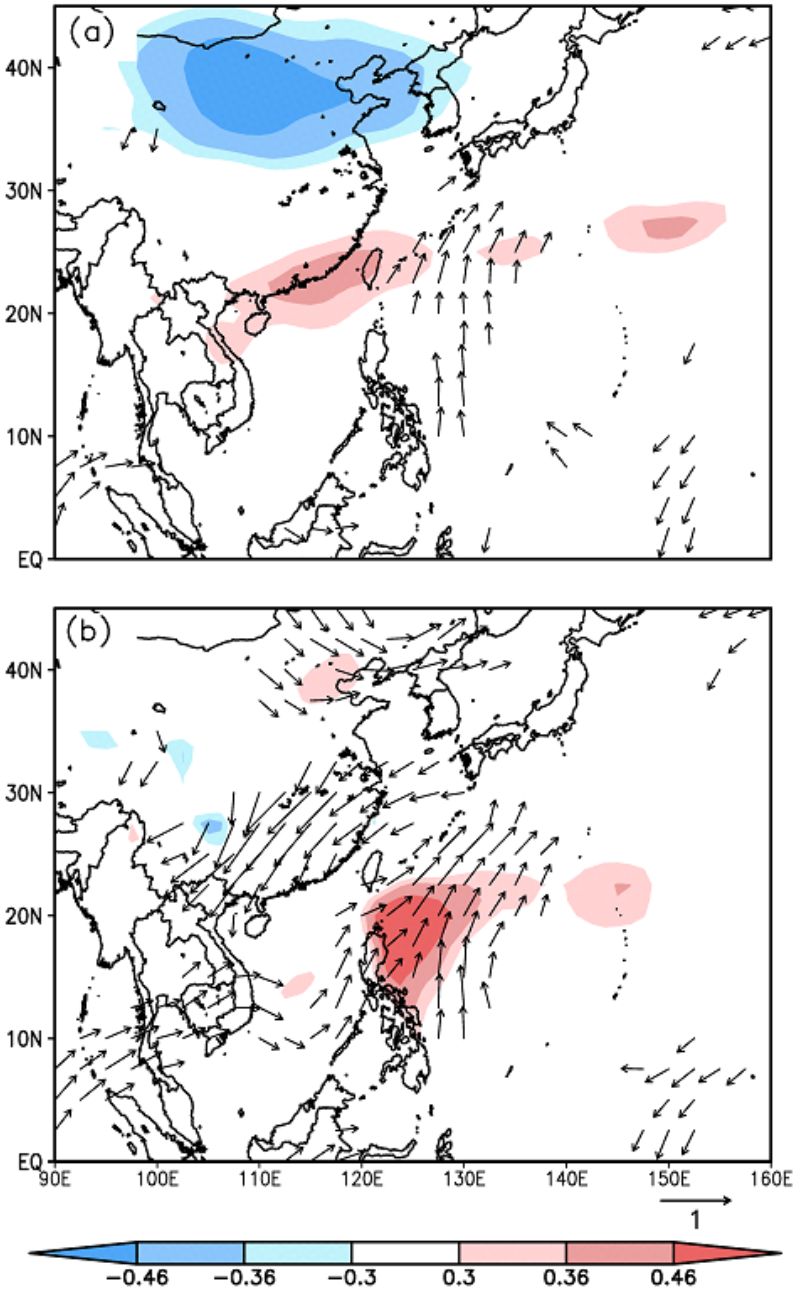

Figure 4.5: Correlation of interannual variations between precipitation of Okinawa region and temperature (shaded), and wind (vector). (a) 500 hPa fields. (b) 850 hPa fields. Shaded where correlation greater than 0.3 is significant at 90 % confidence level.

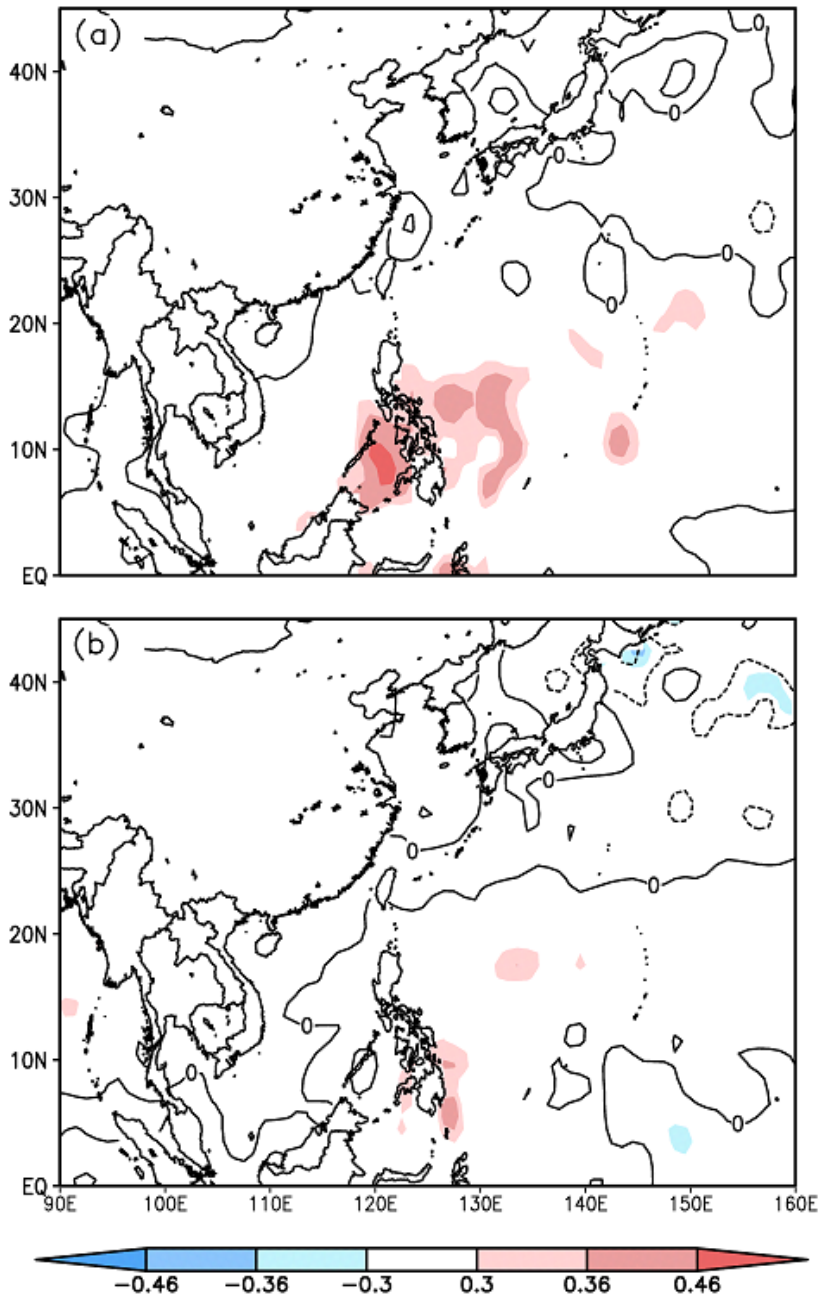

Figure 4.6: Correlation (shaded) and regression (contour) of interannual variations between precipitation of Okinawa region in May and SST (a) in April, and (b) in May. Contour interval is interval 0.05 K. Shaded where correlation greater than 0.3 is significant at 90 % confidence level.

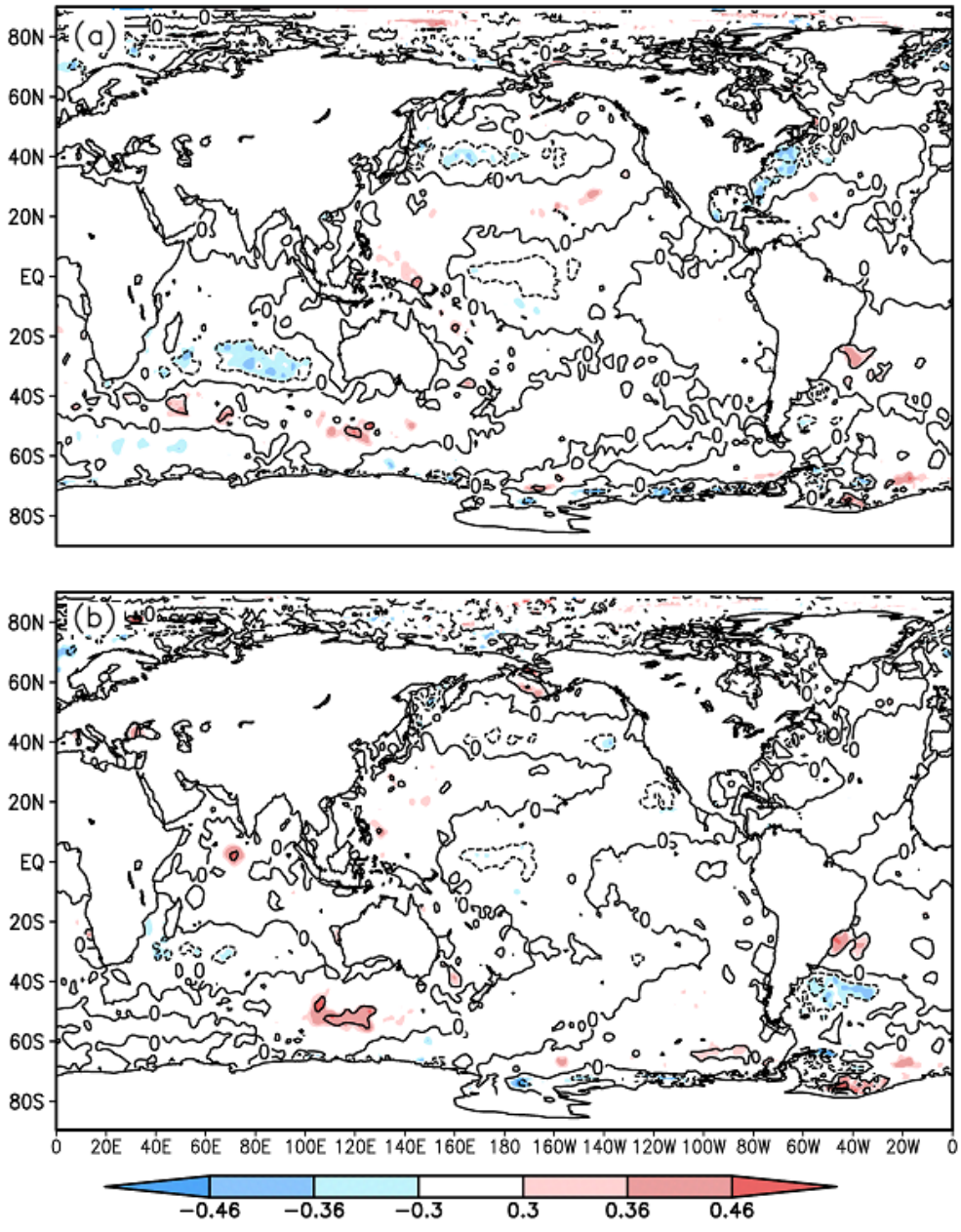

Figure 4.7: Correlation (shaded) and regression (contour) of interannual variations between precipitation of Okinawa region in May and SST of each month (January-June). (a) January. (b) February. Contour interval is interval 0.05 K. Shaded where correlation greater than 0.3 is significant at 90 % confidence level. Same as Figure 4.6 but for global fields.

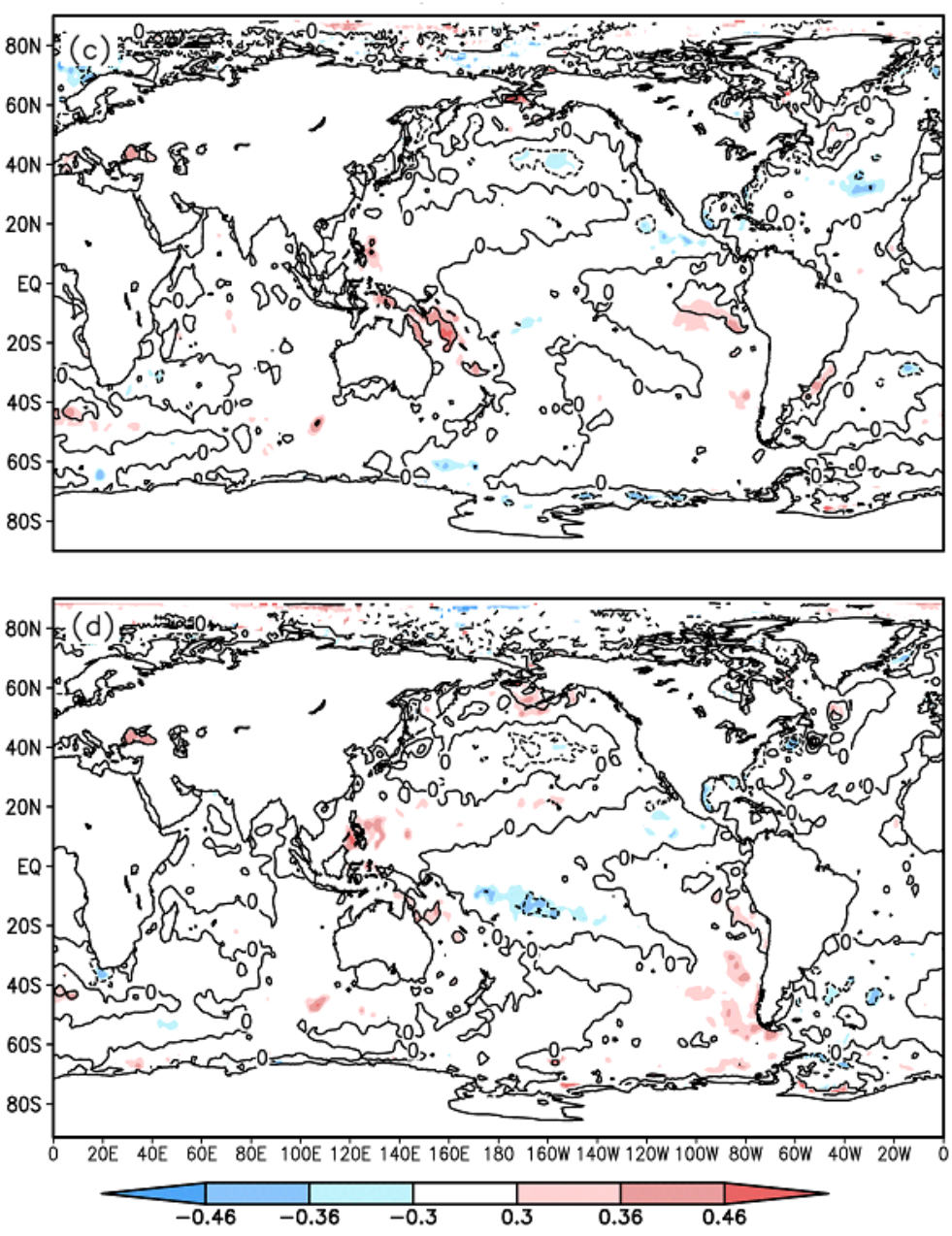

Figure 4.7: (Continued): (c) March. (d) April.

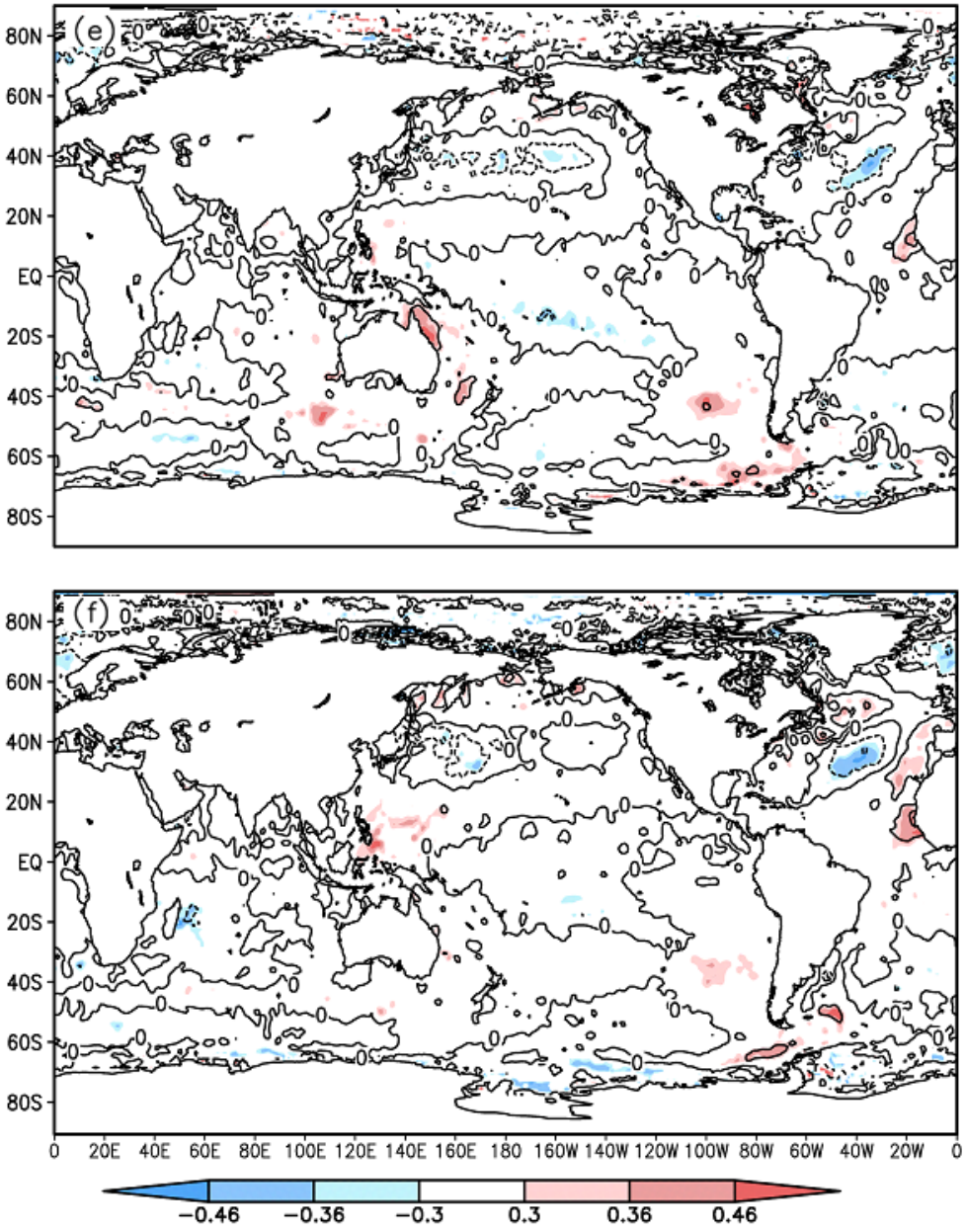

Figure 4.7: (Continued): (e) May. (f) June.

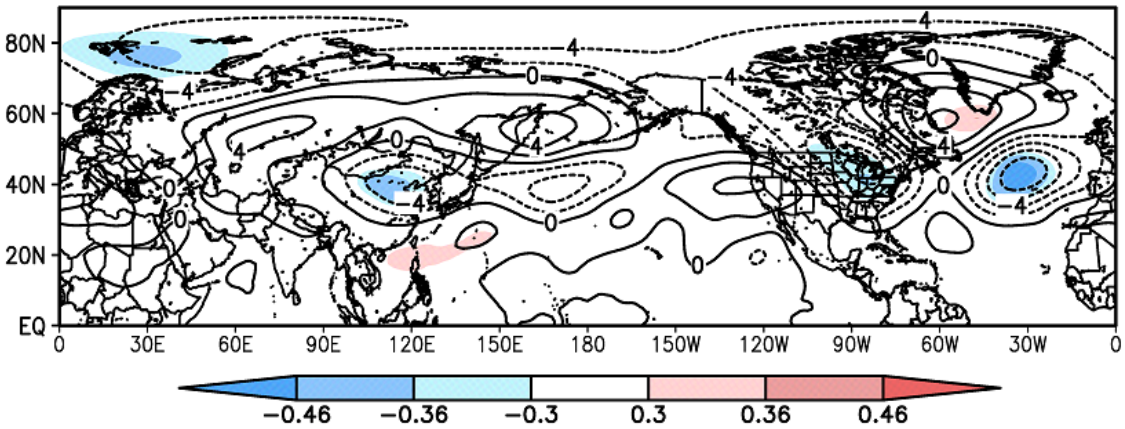

Figure 4.8: Correlation (shaded) and regression (contour) of interannual variability between precipitation of Okinawa region and geopotential height at 200 hPa in May. Contour interval is interval 2 gpm. Shaded where correlation greater than 0.3 is significant at 90 % confidence level.

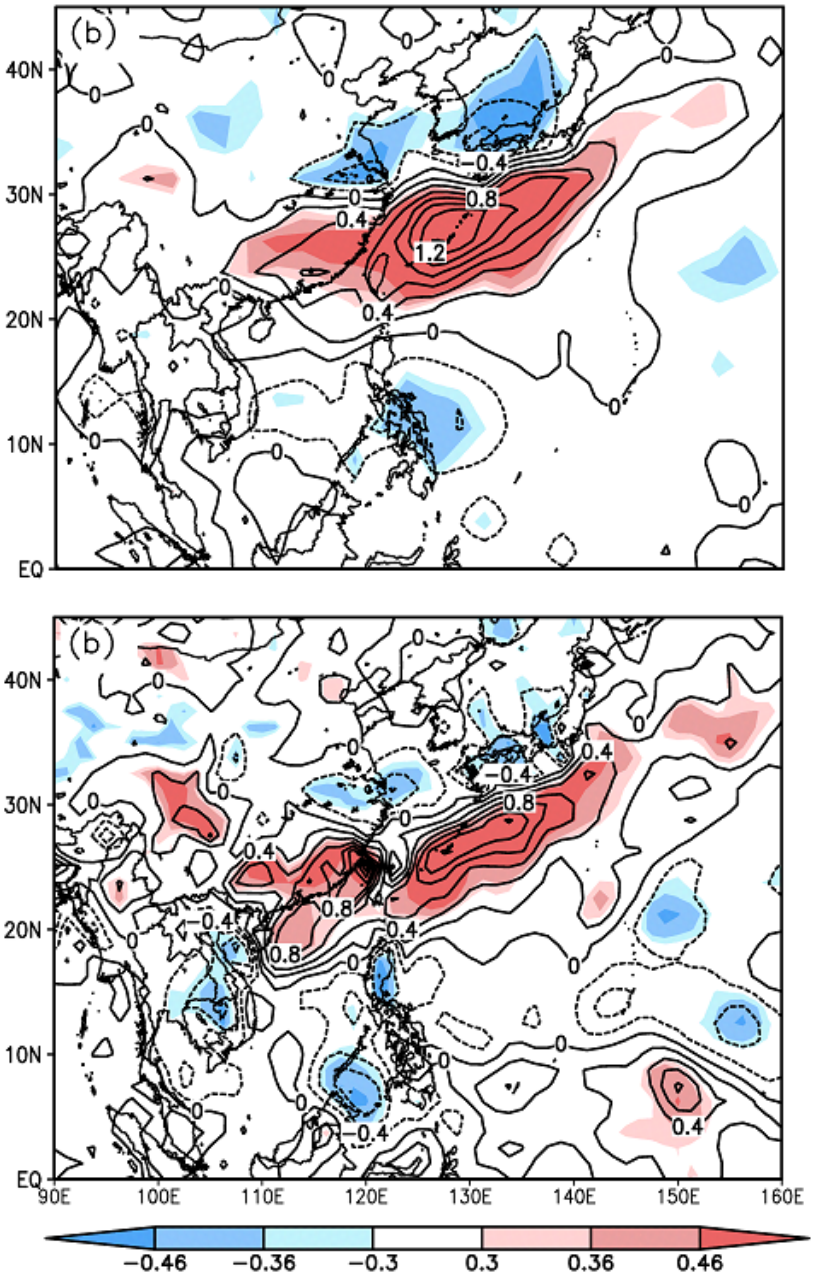

Figure 4.9: Correlation (shaded) and regression (contour) of interannual variability between precipitation of Okinawa region and (a) environmental precipitation, and (b) convergence (positive) / divergence (negative) of moisture flux in June. Contour interval is interval 0.2 mm day^{-1}. Shaded where correlation greater than 0.3 is significant at 90 % confidence level.

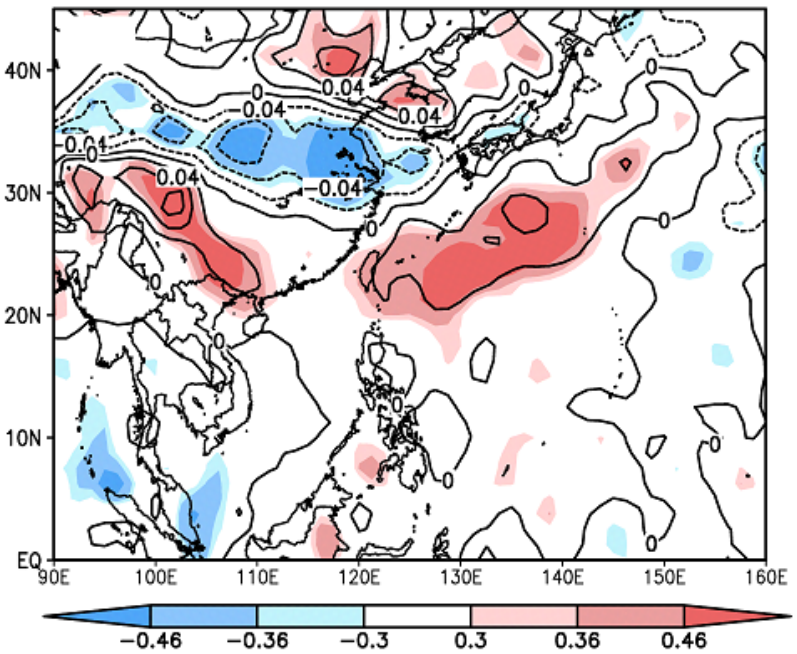

Figure 4.10: Same as Figure 4.8 but for with temperature advection at 500 hPa. Contour interval is 0.02 K day^{-1} with negative contours dashed. Shaded where correlation greater than 0.3 is significant at 90 % confidence level.

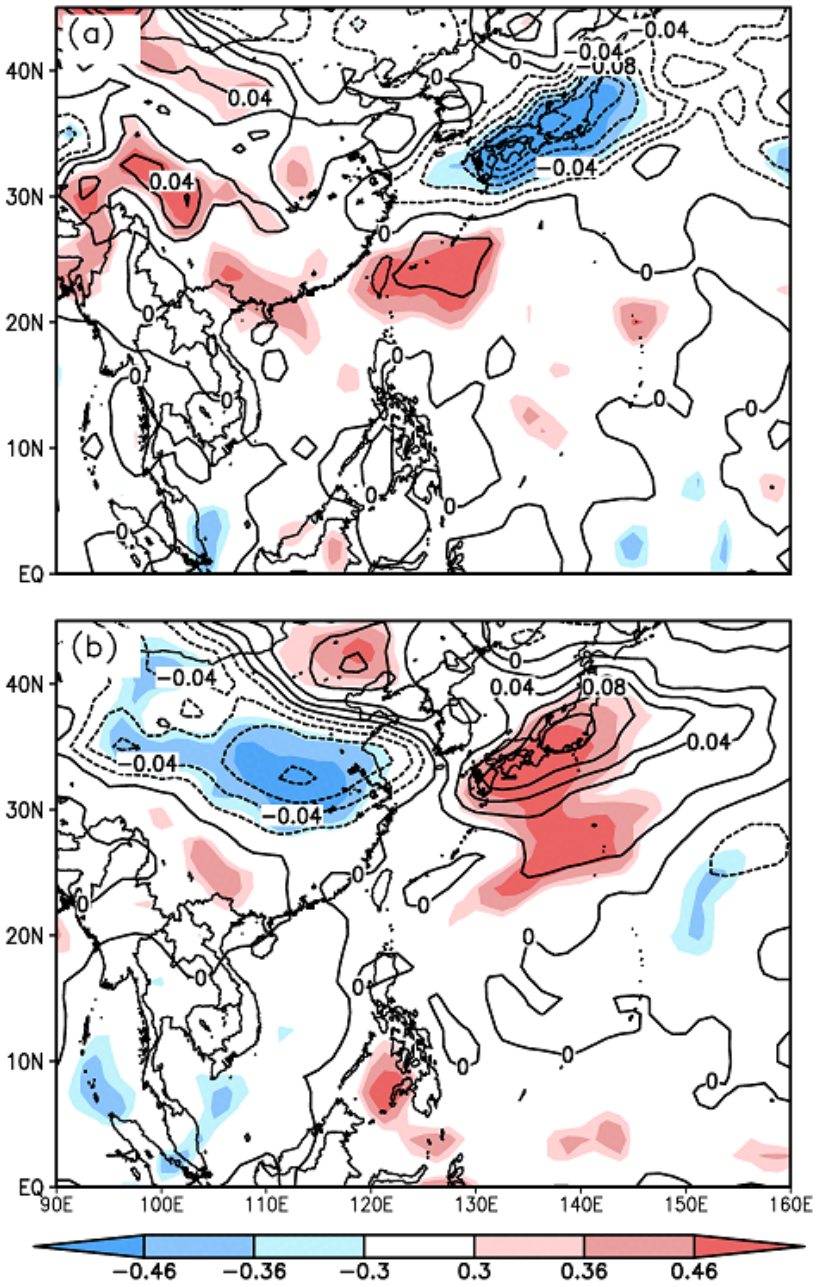

Figure 4.11: Same as Figure 4.9 but for with (a) zonal term, and (b) meridional term of 500-hPa temperature advection. Contour interval is 0.02 K day^{-1} with negative contours dashed. Shaded where correlation greater than 0.3 is significant at 90 % confidence level.

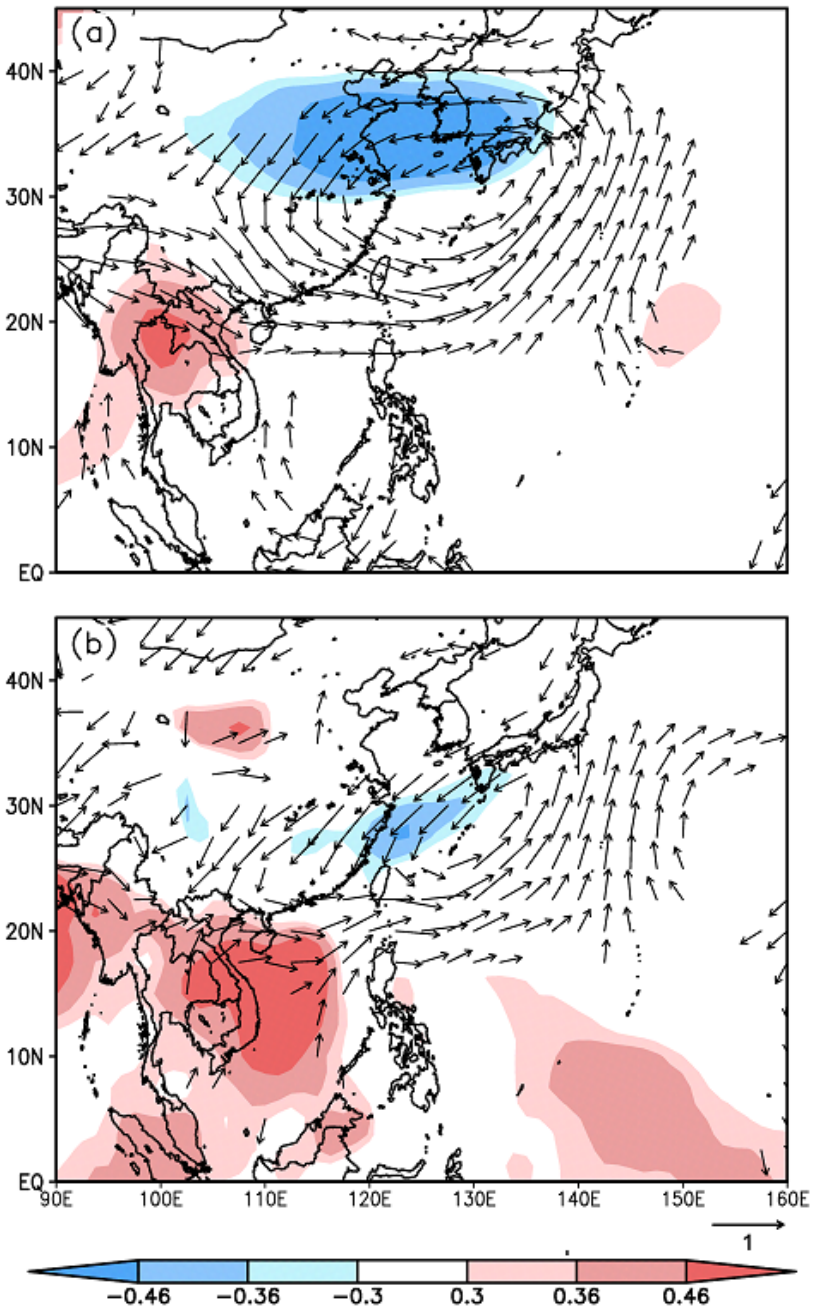

Figure 4.12: Correlation of interannual variations between precipitation of Okinawa region and temperature (shaded), and wind (vector). (a) 500 hPa fields. (b) 850 hPa fields in June. Shaded where correlation greater than 0.3 is significant at 90 % confidence level.

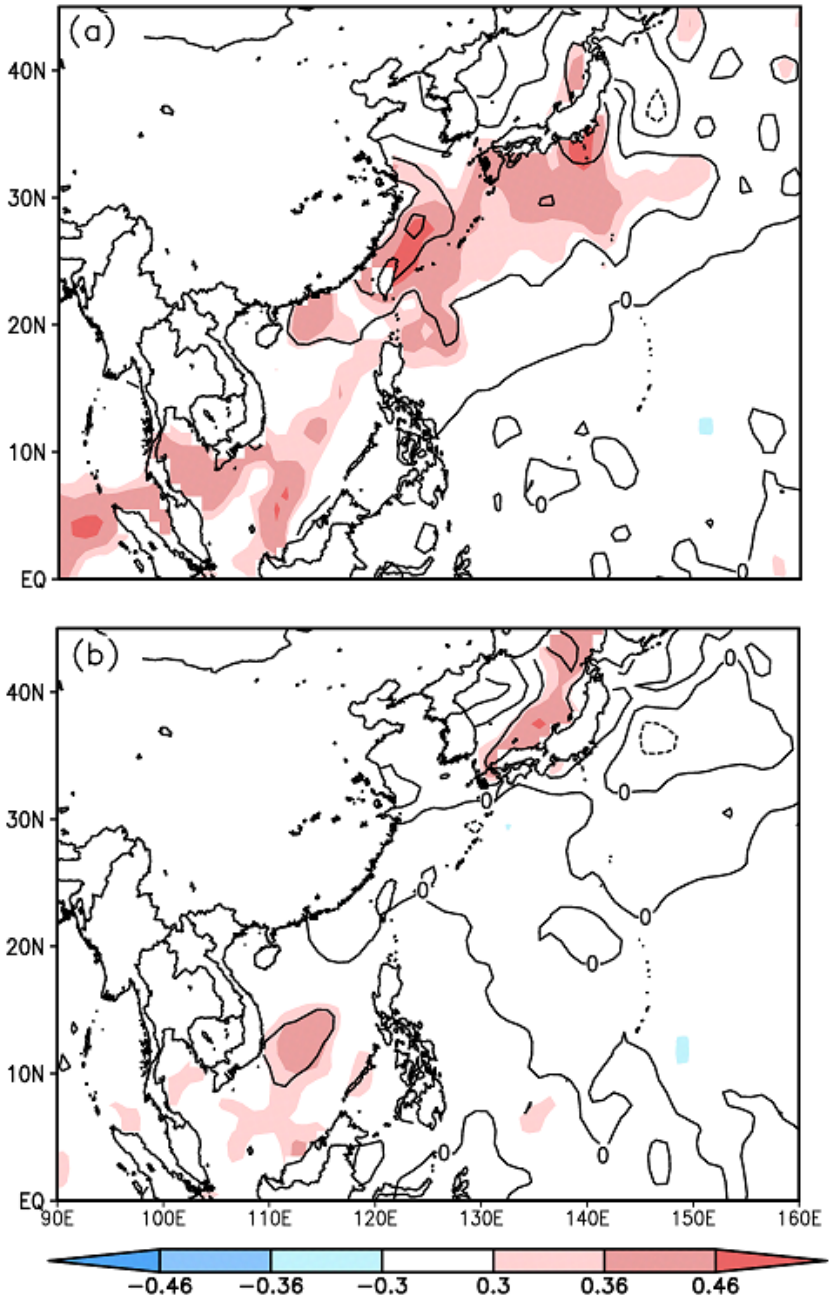

Figure 4.13: Correlation (shaded) and regression (contour) of interannual variability between precipitation of Okinawa region in June and SST (a) in May, and (b) in June. Contour interval is interval 0.05 K. Shaded where correlation greater than 0.3 is significant at 90 % confidence level.

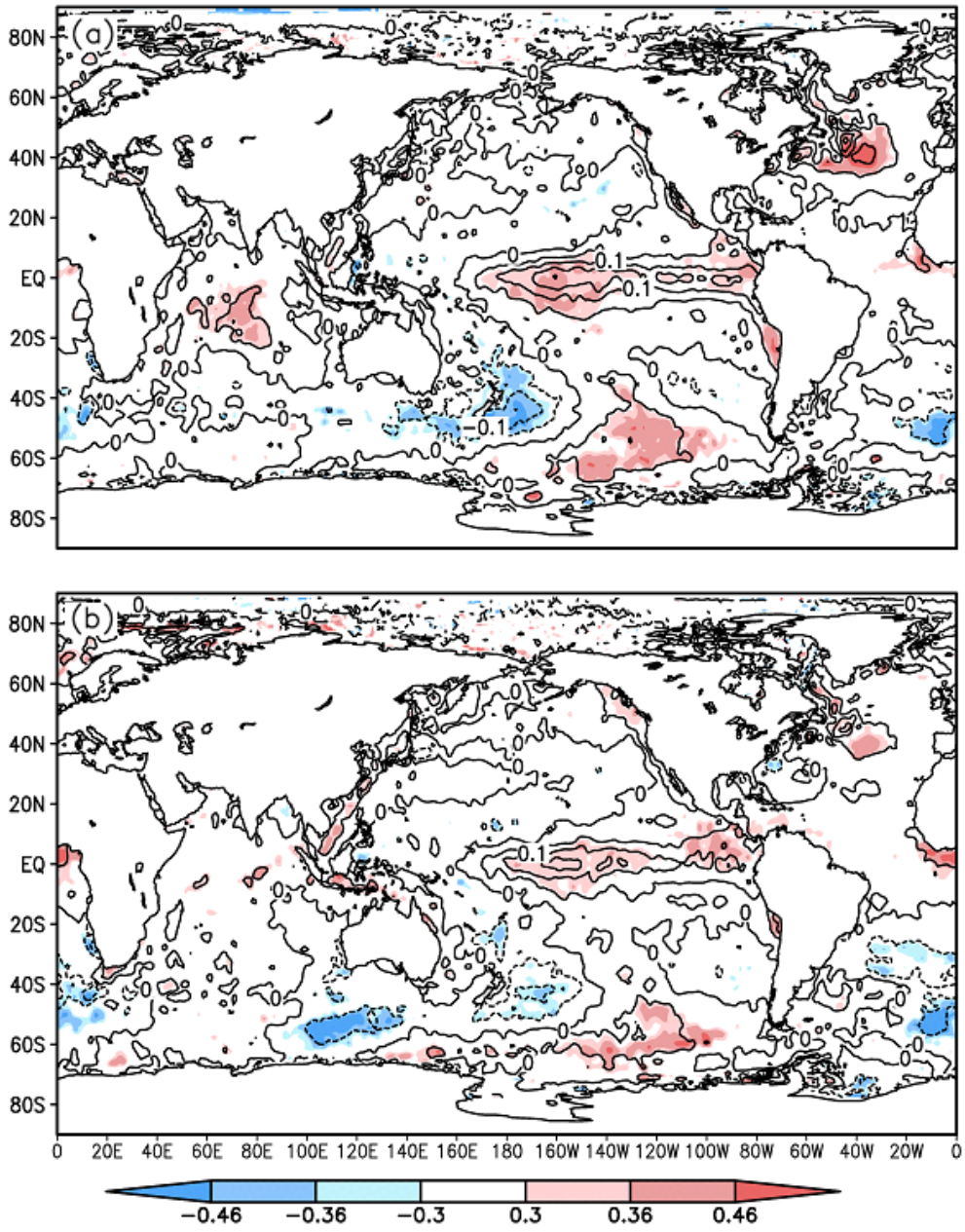

Figure 4.14: Correlation (shaded) and regression (contour) of interannual variability between precipitation of Okinawa region in June and SST of each month. (a) January. (b) February. Contour interval is interval 0.05 K. Shaded where correlation greater than 0.3 is significant at 90 % confidence level. Same as Figure 4.12 but for global fields.

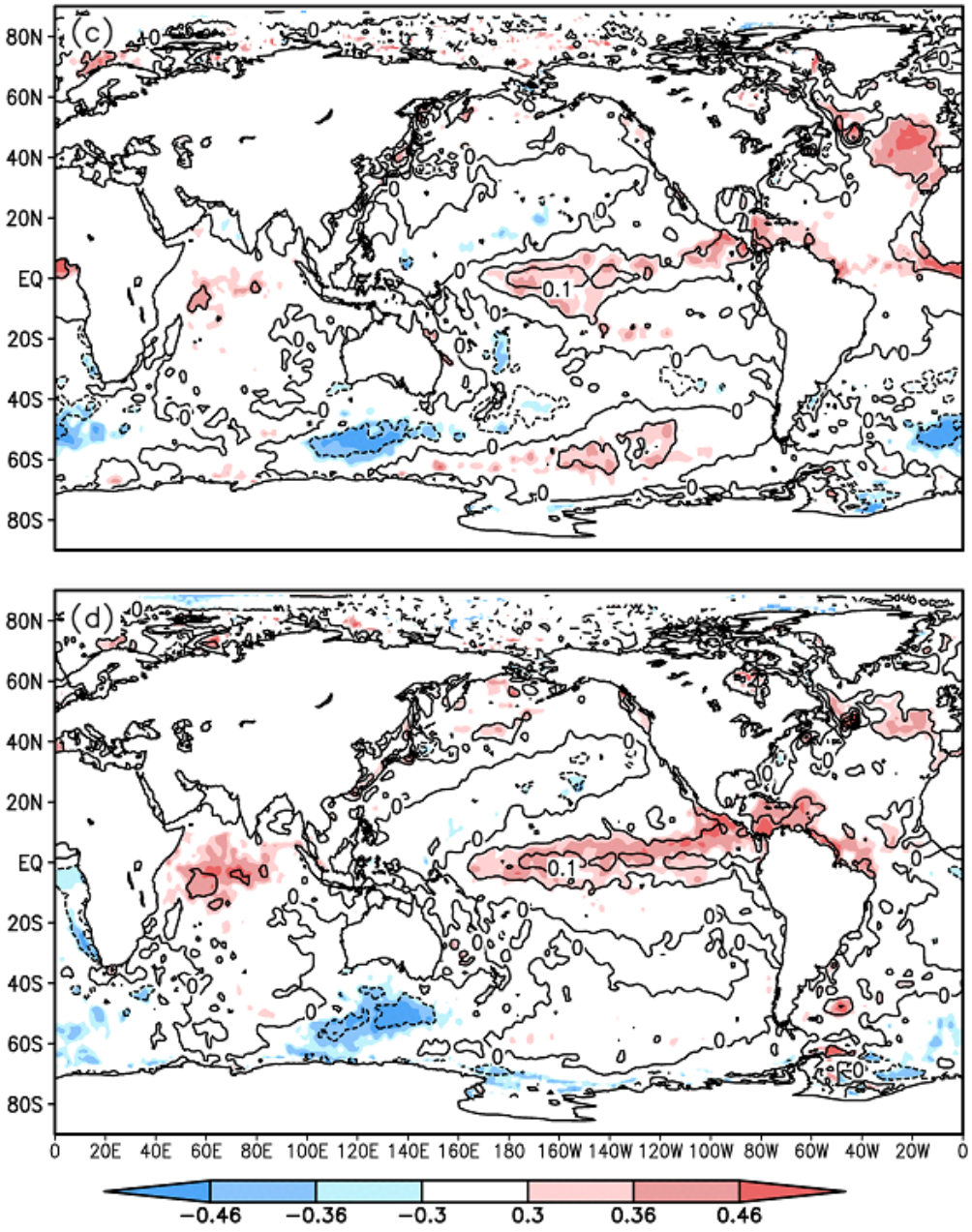

Figure 4.14: (Continued): (c) March. (d) April.

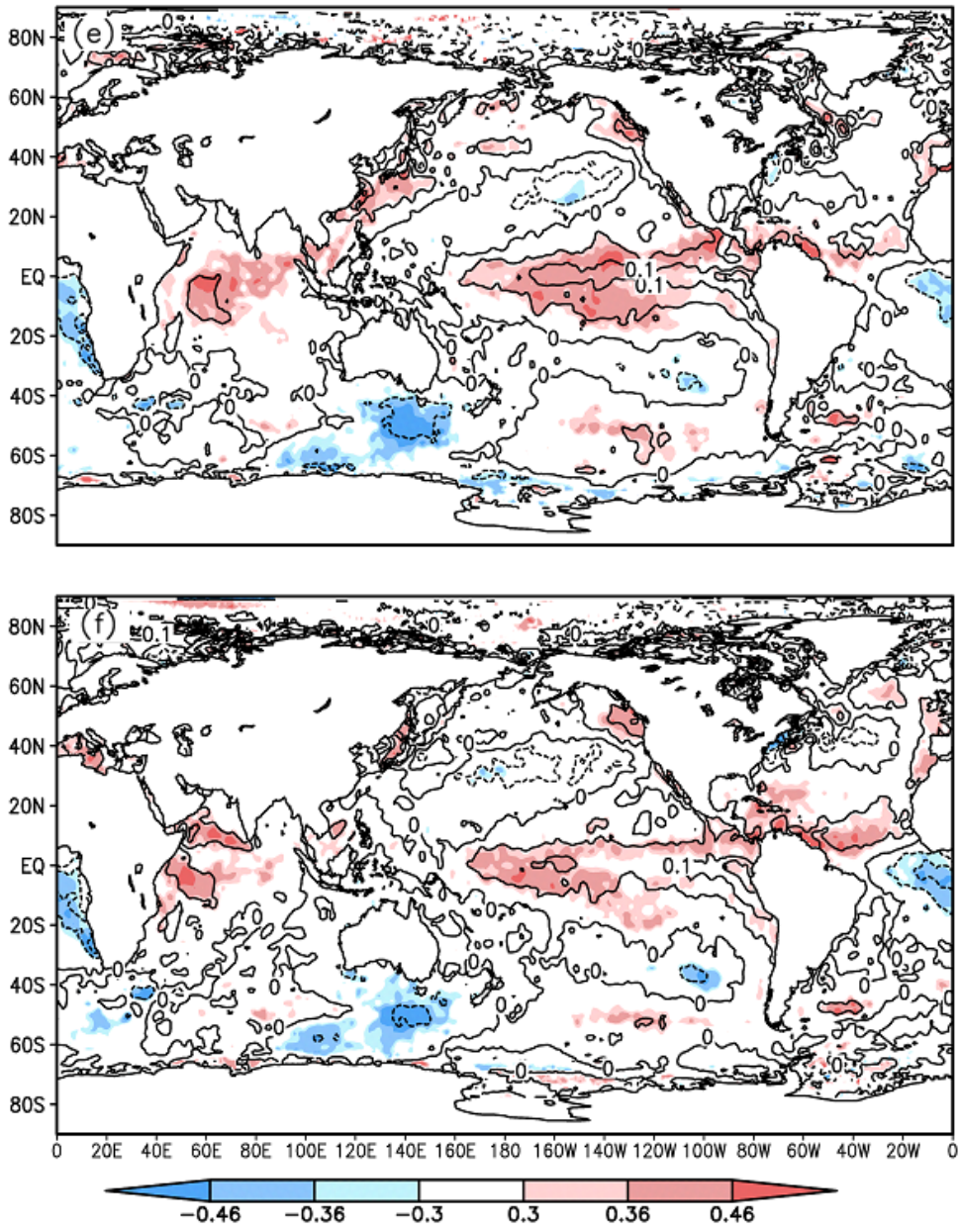

Figure 4.14: (Continued): (e) May. (f) June.

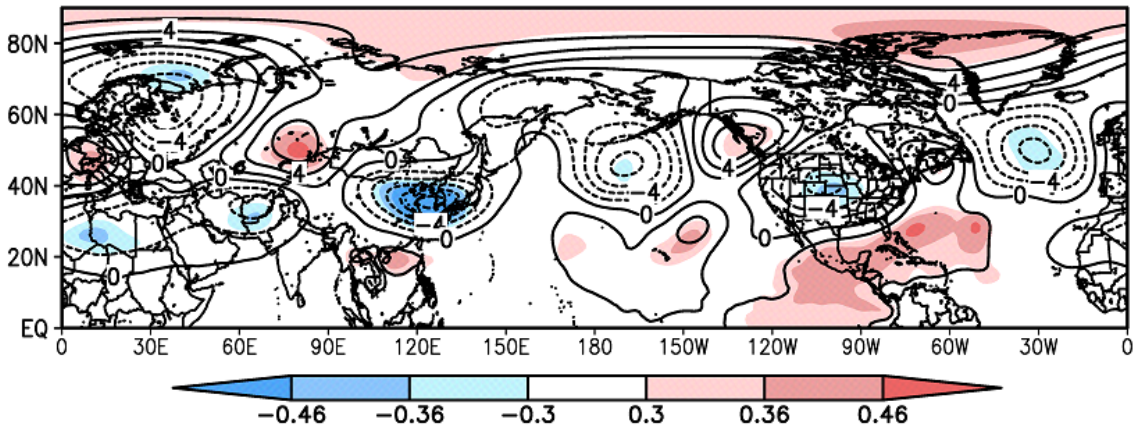

Figure 4.15: Correlation (shaded) and regression (contour) of interannual variability between precipitation of Okinawa region and geopotential height at 200 hPa in June. Contour interval is interval 2 gpm. Shaded where correlation greater than 0.3 is significant at 90 % confidence level.

Chapter 5

Conclusion

We have investigated the detailed climatological evolution of the Okinawa baiu and its interannual variability. The Okinawa baiu season spans May and June, with an initial peak in precipitation during mid-May (Fig. 3.2 and Fig. 3.3a). This initial peak is explained by a strong north–south temperature gradient at 500 hPa and northward winds in the vicinity of Okinawa. These two factors together produce warm advection and upward motion over Okinawa during mid-May (Fig. 3.10). Precipitation over Okinawa is reduced during late May when the baiu front shifts southeastward (Figs 3.3 and 3.4e-f). A region of cold advection from the north shifts southward to cover the northern part of Okinawa during this period (Figs. 3.7c and 8b). We suggest a possibility that the southward migration of this region of cold advection causes a short break in the Okinawa baiu that coincides with the onset of the South China Sea (SCS) monsoon. Another possibility is that the SCS monsoon affects the Okinawa baiu, which will be discussed later. A strong east–west temperature gradient develops at 500 hPa during June. Together with westerly winds, this east–west temperature gradient leads to strong warm advection in the zonal direction (Fig. 3.10). This warm advection induces the baiu rainband to return to the Okinawa region. The region of strong warm advection shifts northward from Okinawa in late June, and the Okinawa baiu withdraws.

Our results are broadly consistent with the warm temperature advection mechanism proposed by Sampe and Xie (2010). The behavior of the baiu rainband in the Okinawa region can be explained by seasonal variability in horizontal temperature advection at 500 hPa. The second peak of Okinawa baiu precipitation in June represents a southward extension of the mainland Japan baiu, which withdraws in late June when the region of strong warm advection shifts northward (Figs 3.3b and 3.5b).

We have also investigated the evolution of transient eddy disturbances during the May–June period. Typhoon is one of transient disturbances. The mid-May peak in mean precipitation amount excluding typhoon days is approximately 20% less than the 10-year mean; however, the peak in mean precipitation amount during June changes little relative to the 10-year mean (Fig. 3.13). In general, the evolution of transient eddy activity corresponds well to the evolution of the Okinawa baiu. Transient eddy activity is stronger during May than during June, and probably contributes to the peak in precipitation in mid-May.

The baiu rainband is situated around Okinawa and displays a large interannual variation during baiu period. That is evident in time-series of precipitation during Okinawa baiu for 10-year (Figs. 3.1 and 3.2). Whereat, finally, we have investigated interannual variations in the Okinawa baiu using JRA-25 data and GPCP monthly precipitation data over a longer time period (1979–2008). Precipitation in May is correlated with 500-hPa weak warm temperature advection and 500-hPa cold temperature to the north of Okinawa and warm temperature to the south China (Figs. 4.3 and 4.5a). Additionally, it is also correlated with southerly wind to the northeast Philippines (Fig. 4.5a). In June, precipitation is correlated with 500-hPa warm advection to the southeast of Okinawa, such as it is relation with the westward warm Indochina

and westerly wind (Figs. 4.10 and 4.12).

Precipitation in June is correlated with the SST around Okinawa in previous month, i.e., May (East China Sea and south of Japan) and equatorial east Pacific (Figs. 4.13a and 4.14). Okinawa baiu in June is enhanced in the El Nino years, while that in May has no correlation with ENSO. The ENSO brought about the PJ pattern, which affect the baiu rainfall in mainland Japan. However, the Okinawa baiu rainfall does not seen to be related with the PJ pattern (Fig. 4.15).

These results support our interpretations of differences between large-scale features associated with the Okinawa baiu in May and those associated with the Okinawa baiu in June.

References

Chan, J. C. L., Y. Wang, and J. Xu, 2000: Dynamic and thermodynamic characteristics associated with the onset of the 1998 South China Sea summer monsoon. *J. Meteor. Soc. Japan,* **78,** 367–380.

Chen, T. –C., S. –Y. Wang, W. –R. Hung, and M. –C. Yen, 2004: Variation of the East Asian Summer Monsoon Rainfall. *J. Climate*, **17,** 744-762.

Fujibe, F., 2006: A short dry period preceding the onset of Baiu over the Honshu-Kyushu region (in Japanese). *Tenki*, **53,** 785–790.

Hirasawa N., K. Kato, and T. Takeda, 1995: Abrupt change in the characteristics of the cloud zone in subtropical East Asia around the middle of May. *J. Meteor. Soc. Japan*, **73,** 221-239.

Hirota, N., and M. Takahashi, 2012: A tripolar pattern as an internal mode of the East Asian summer monsoon. *Clim. Dun*., in press.

Huffman, G. J., R. F. Adler, M. Morrissey, D.T. Bolvin, S. Curtis, R. Joyce, B McGavock, and J. Susskind, 2001: Global precipitation at one-degree daily resolution from multi-satellite observations. *J. Hydrometeor*, **2,** 36–50.

Huang, R., W. Chen, B. Yang, and R. Zhang, 2004: Recent advances in studies of the interaction between the East Asian winter and summer monsoons and ENSO cycle. *Adv. Atmos. Sci.*, **21,** 407-424.

Ishigaki, K., 1982: Baiu (in Japanese). *Technical Report of the Japan Meteorological Agency*, **102**, 103-113.

Kato, K., 1985: On the abrupt change in the structure of the Baiu front over the China

continent in late May of 1979. *J. Meteor. Soc. Japan*, **63,** 20–36.

Kato, K., and Y. –M. Kodama, 1992: Formation of the quasi-stationary Baiu front to the south of the Japan islands in early May of 1979. *J. Meteor. Soc. Japan*, **70,** 631-647.

Kodama, Y.-M., 1992; Large-scale common features of subtropical precipitation zones (the Baiu frontal zone, the SPCZ, and the SACZ). Part 1: Characteristics of subtropical frontal zones. *J. Meteor. Soc. Japan*, **70,** 813-836.

Kosaka, Y., and H. Nakamura, 2010: Mechanisms of Meridional Teleconnection Observed between a Summer Monsoon System and a Subtropical Anticyclone. Part 1: The Pacific-Japan Pattern. *J. Climate*, **23,** 5085-5108.

Kosaka, Y., S. –P. Xie, and H. Nakamura, 2011: Dynamics of Interannual Variability in Summer Precipitation over East Asia. *J. Climate*, **24,** 5435-5453.

Matsumoto, J., 1992: The seasonal changes in Asian and Australian monsoon regions. *J. Meteor. Soc. Japan*, **70,** 257-273.

Matsumoto, J., 1997: Seasonal transition of summer rainy season over Indochina and adjacent monsoon region. *Advances in Atmospheric Sciences*, **14,** 231-245.

Matsumoto, J., and S. Yamamoto, 2009: Rainy seasons in the Nansei-Shotou (Southwest Islands) of Japan. *Geographical Reports Tokyo Metropolitan University*, **44,** 71-78.

Matsumoto, S., K. Ninomiya, and S. Yoshizumi, 1971: Characteristic features of Baiu front associated with heavy rainfall. *J. Meteor. Soc. Japan*, **49,** 267–281.

Ninomiya, K., and H. Muraki, 1986: Large-scale circulations over East Asia during Baiu period of 1979. *J. Meteor. Soc. Japan*, **64,** 409–429.

Ninomiya, K., and T. Akiyama, 1992: Multi-scale features of Baiu, the summer monsoon over Japan and the East Asia. *J. Meteor. Soc. Japan*, **70,** 467–495.

Ninomiya, K., and Y. Shibagaki, 2007; Multi-scale features of the Meiyu-Baiu front and

associated precipitation systems. *J. Meteor. Soc. Japan*, **85B**, 103-122.

Nitta, T., 1987: Convective activities in the tropical western Pacific and their impact on the Northern Hemisphere summer circulation. *J. Meteor. Soc. Japan*, **65**, 373-390.

Onogi, K., J. Tsutsui, H. Koide, M. Sakamoto, S. Kobayashi, H. Hatsushika, T. Matsumoto, N. Yamazaki, H. Kamahori, K. Takahashi, S. Kadokura, K. Wada, K. Kato, R. Oyama, T. Ose, N. Mannoji, and R. Taira, 2007: The JRA-25 Reanalysis. *J. Meteor. Soc. Japan*, **85,** 369–432.

Rayner, N. A., D. E. Parker, E. B. Horton, C. K. Folland, L. V. Alexander, D. P. Rowell, E. C. Kent, and A. Kaplan, 2003: Global analyses of sea surface temperature, sea ice, and night marine air temperature since the late nineteenth century. *J. Geophys. Res.* Vol. **108,** No. D14, 4407, doi:10.1029/2002JD002670.

Reynolds, R. W., T. M. Smith, C. Liu, D. B. Chelton, K. S. Casey and M. G. Schlax, 2007: Daily High-resolution Blended Analyses for sea surface temperature. *J. Climate*, **20,** 5473-5496.

Reynolds, R. W., 2008: What's New in Version 2. *OISST Webpage*.

Sampe, T., and S. -P. Xie, 2010: Large-scale dynamics of the Meiyu-Baiu rainband: environmental forcing by the westerly jet. *J. Climate*, **23,** 113–134.

Takahashi, K., N. Yamazaki, and H. Kamahori, 2006: Trends of heavy precipitation events in global observation and reanalysis datasets. *SOLA*, **2,** 96–99.

Tanaka, H., 2007: The meteorology of westerlies (in Japanese). *Seizando*, 174pp.

Tanaka, M., 1992: Intraseasonal oscillation and the onset and retreat dates of the summer monsoon over East, Southeast Asia and the Western Pacific Region using GMS high cloud amount data. *J. Meteor. Soc. Japan*, **70,** 613–629.

Tanaka, M., 1997: Interannual and interdecadal variations of the western North Pacific

monsoon and Baiu rainfall and their relationship to the ENSO cycles. *J. Meteor. Soc. Japan*, **75,** 1109-1123.

Tian, S. –F., and T. Yasunari, 1998: Climatological aspects and mechanism of spring persistent rains over central China. *J. Meteor. Soc. Japan*, **78,** 57-71.

Tomita, T., T. Yoshikane, and T. Yausnari, 2004: Biennial and lower-frequency variability observed in the early summer climate in the western North Pacific. *J. Climate*, **17,** 4254-4266.

Ueda H., T. Yasunari, and R. Kawamura, 1995: Abrupt seasonal change of large-scale convective activity over the western Pacific in the northern summer. *J. Meteor. Soc. Japan*, **73,** 795-809.

Ueda, H., and M. Ohba, 2009: Important factors for the development of the Asian-Northwest Pacific summer monsoon. *J. Climate*, **22,** 649–669.

Wang, B., LinHo, Y. Zhang, and M. -M. Lu, 2004: Definition of South China Sea Monsoon onset and commencement of the East Asia summer monsoon. *J. Climate*, **17,** 699–710.

Watanabe, M., and M. Kimoto, 2000: Atmosphere-ocean thermal coupling in the North Atlantic: A positive feedback. *Quart. J. Roy. Meteor. Soc.*, **126,** 3343-3369.

Watarai, Y., and H. L. Tanaka, 2007: Characteristics of the JRA-25 dataset from the viewpoint of global energetics. *SOLA*, **3,** 9–12.

Yatagai, A., O. Arakawa, K. Kamiguchi, H. Kawamoto, M. I. Nodzu, and A. Hamada, 2009: A 44-year daily gridded precipitation dataset for Asia based on a dense network of rain gauges. *SOLA*, **5,** 137–140, doi:10.2151/sola.2009-35.